The impact of UVC and VUV treatment on the toxicity, leaching and degradation of tire rubber microplastic

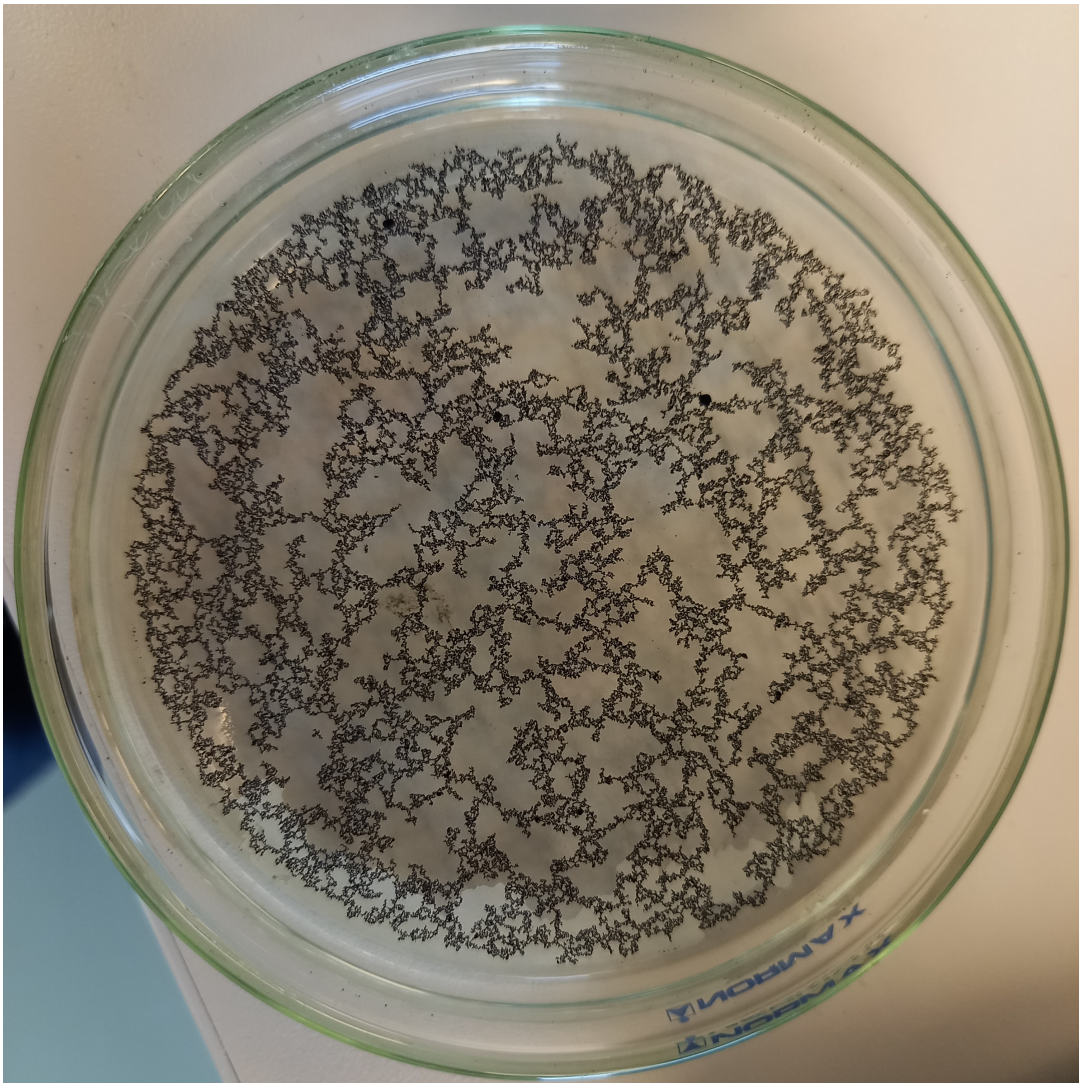

Master Thesis
9th and 10th semester

Environmental Science, cand.tech.

Aalborg University
10.06.2022

Department of Chemistry and Bioscience
Environmental Science
Frederiks Bajers Vej 7H
9220 Aalborg Øst

Title:

The impact of UVC and VUV treatment on the toxicity leaching and degradation of tire rubber microplastic.

Project:

Master Thesis (60 ECTS)

Project Period:

September 2021 - June 2022

Student:

Emil Bock Nielsen

Supervisor:

Peter Roslev

Total number of pages: 58
Appendix pages: 6
Project ended: 10-06-2022

Abstract:

Microplastic is an increasingly persistent pollutant in the aquatic and terrestrial environment. An often overlooked source of microplastics is tire rubber microplastics (TRMP). It is estimated that an average of 0.81 $\frac{kg}{year}$ is emitted per capita globally. The rubber particles are transported with road runoff to waste water treatment plants where they might be exposed to UV irradiation used in microbial disinfection. This study investigates the effects that UV irradiation have on the toxic compounds leaching from tire rubber particles. TRMP particles suspended in tapwater and particle free leachates are treated with two different types of UV light, 254 nm UVC and a mix of 254 nm and 185 nm VUV in a collimated beam setup, at different durations of exposure. As a measure of toxicity, the model organism *Raphidocelis subcapitata* was exposed to leachates from non treated particles and particles treated with UVC and VUV/UVC. The toxic compounds in the leachates were measured as concentrations of zinc and the PAHs fluoranthene, pyrene and benzo(a)pyrene. The results of the growth inhibition showed that, both UVC and VUV/UVC promote the leaching of toxic compounds from TRMP particles. The results also showed that UVC and VUV/UVC removed toxic compounds from TRMP leachates, with VUV/UVC being more effective. UVC removed 66% of the measured PAHs from TRMP leachate, while VUV/UVC removed 88% of the measured PAHs. The findings in this study shows the potential of VUV/UVC as a way to mitigate the load of toxic compounds leaching from TRMP into the environment.

Table of Contents

Acknowledgements

I would like to show my appreciation to my supervisor, Peter Roslev at the Department of Chemistry and Bioscience at Aalborg University for guidance and feedback during the whole process. I would also like to thank Peter Vittrup Christensen from ULTRAAQUA for supplying the collimated beam setup used for VUV treatment. Laboratory assistance from laboratory technician Helle Blendstrup and research assistant Lana Flanjak was greatly appreciated. Lastly, I would like to thank my girlfriend Indra Pētersone for her unconditional support and motivation during my studies.
Emil Bock Nielsen
10.06.2022

Glossary of terms

ELT - End of Life Tire
EPA - Environmental Protection Agency
ETRMA - European Tyre and Rubber Manufacturers Association
ISO - International Organization for Standardisation
MP - Microplastics
PAH - Polycyclic Aromatic Hydrocarbon
PM - Particulate matter
REACH - Registration, Evaluation, Authorisation and Restriction of Chemicals
TRMP - Tire Rubber Microplastic
TWP - Tire Wear Particles
UV - Ultraviolet light (400-10 nm)
UVA - Ultraviolet A (400-315 nm)
UVB - Ultraviolet B (315-280 nm)
UVC - Ultraviolet C (280-200 nm)
VUV - Vacuum Ultraviolet (200-100 nm)
WWTP - Waste Water Treatment Plant

1 Introduction

The world produces increasingly more plastic every year. Despite the COVID-19 pandemic the global plastic production only saw a 0.3 % decrease in 2020 (367 million tons) compared to the previous year 2019 (368 million tons) [PlasticsEurope, cited October 2021]. As a consequence of this more and more plastic pollution finds its way into the terrestrial, freshwater and marine environment every year. Microplastic have in recent years been studied as an environmental pollutant that could have potential harming impacts on the environment [Lassen et al., 2015]. Microplastics are pieces of plastic in the size range 5 mm down to 1 μm. Above this size range it is considered macroplastic and plastic particles smaller than 1 μm are considered as nanoplastics [Evangeliou et al., 2020]. Most micro- and nanoplastic in the environment stems from larger pieces of plastic fragmented into smaller sizes via physical abrasion, photodegradation, hydrolysis and biodegradation [Gewert et al., 2015]. These plastics are defined as secondary microplastics, as opposed to primary microplastics which are plastics used intentionally in sizes between 1 μm and 5 mm, in fx. in cosmetics, paint or as a raw material for plastic and rubber production [Lassen et al., 2015].

A major source of microplastic pollution is tire wear particles (TWP). It is estimated by Kole et al. [2017] that 6.1 million tons of TWPs are emitted to the environment every year globally. The emmisions per capita range from 0.23 to 4.7 $\frac{kg}{year}$ with a global average of 0.81 $\frac{kg}{year}$ [Kole et al., 2017]. 3-7% of airborne particulate matter ($PM_{2.5}$) is estimated to come from tire wear, indicating a potential contribution to the global health burden of air pollution [Kole et al., 2017]. Airborne TWP have also been shown to be able to travel far distances in the atmosphere and be deposited in the world ocean or in the Arctic region where the light-absorbing properties of TWP could cause accelerated warming and melting of the cryosphere [Evangeliou et al., 2020].

The Danish Environmental Protection Agency (Miljøstyrelsen) have estimated that 60.2 % of all microplastic pollution from Danish sources stems from car tires (see figure 1) and that between 500 and 1,700 tons of tire rubber particles per year end up in the aquatic environment in Denmark [Lassen et al., 2015].

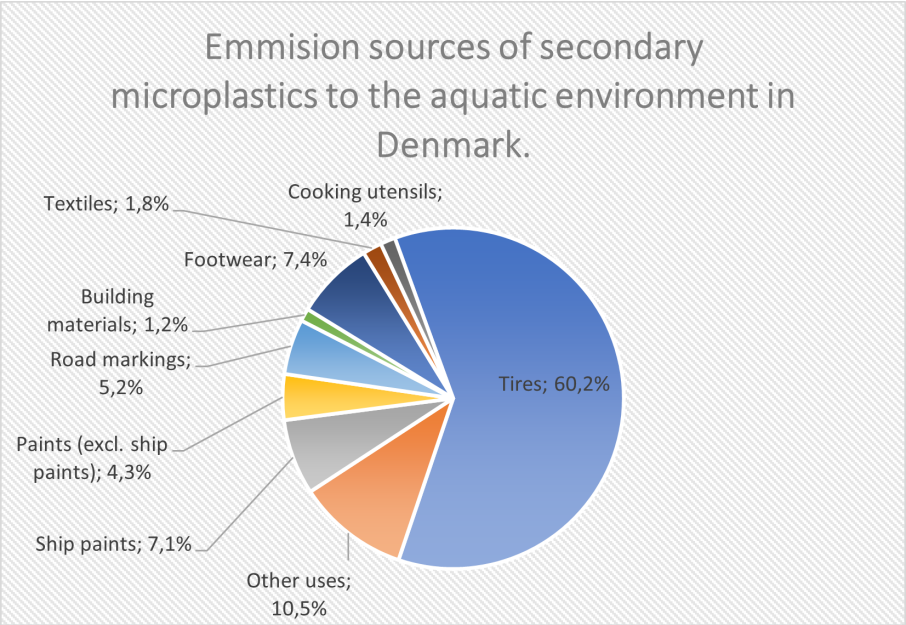

Figure 1. Sources of secondary microplastic to the aquatic environment in Denmark, sources of macro plastic that later degrades to microplastics are not included. Data from Lassen et al. [2015].

Tire rubber contains substances that can leach out into the environment and be toxic to flora and fauna in the terrestrial and aquatic environment [Wik, 2007]. These substances include various Polycyclic Aromatic Hydrocarbons (PAH) and Zinc and have been shown to have negative effects on the aquatic environment [Lu et al., 2021; Rhodes et al., 2012; Wik, 2007; Wik and Dave, 2006]. One study have even found of that of all plastics investigated, leachates from car tire rubber had the biggest toxicological effect on the various organisms investigated [Capolupo et al., 2020].

Degradation of microplastics in the environment is very slow and can take up to hundreds or even thousands of years [Zhang et al., 2021]. Plastics is however degraded through various mechanical, chemical and biological pathways. One of the main degradation pathways are through photodegradation [Zhang et al., 2021]. Photodegradation mostly happens by the exposure to ultraviolet (UV) radiation from the sun. The wavelengths reaching the atmosphere are in the range of UVA (400-315 nm) and UVB (315 - 280 nm) irradiation. Therefore most studies investigating photodegradation of plastics uses these UV types to simulate natural degradation [Zhang et al., 2021].

A considerable amount of microplastics eventually end up going through a waste water treatment plant (WWTP). While most of the microplastic is removed during the mechanical removal and sedimentation processes in the WWTP, smaller particles are still making their way through to the aquatic environment [Murphy et al., 2016]. UVC (280-200 nm) and vacuum UV (VUV) (200-100 nm) are being used more and more as a part of the disinfection of both wastewater and drinking water to inactivate different bacteria and viruses in the effluent or to remove total organic carbon (TOC) in industrial wastewater [Zewde et al., 2020; Naderi et al., 2017]. Due to these technologies being used in the relation to waste water it is interesting to investigate how these shorter wavelengths of UV

affect the microplastic particles [Lin et al., 2020]. One study has shown that UVC and VUV have altering effects on the surface morphology of select microplastics [Lin et al., 2020]. There is still a lack of studies showing the effects that these types of UV radiation can have on tire rubber microplastic and to what extend it will affect the release of toxic chemicals from the rubber to the aquatic environment.

1.1 Problem Statement

As stated previously, tire rubber microplastic (TRMP) is a large fraction of microplastics in the aquatic environment. It is unclear what effect these particles impose on the aquatic environment. With the inclusion of UVC and VUV in various water treatment technologies the effects of these treatments on microplastic particles are worth investigating to better asses the impact these particles have on the environment. This study will aim to do the following:

Investigate the effects that UVC and VUV/UVC irradiation have on the leaching of toxic compounds from TRMP particles and the effects that UVC and VUV/UVC irradiation have on the removal of these compounds from the water.

The specific aims of this study are therefore:

- Measuring the effects UVC and VUV light have on the leaching of toxic compounds from tire rubber microplastics and the potential mitigating effects from these treatments.
- Comparing the difference in toxicity between treated and non UV treated tire rubber microplastics.
- Analysing, comparing and quantifying the compounds released from tire rubber microplastics both non-treated and treated with UV light.
- Investigating the potential mitigating effects UVC and VUV treatment have on leachates (PAH and zinc) from tire rubber microplastic.

2 Theory

2.1 Tire rubber microplastic in the environment

Microplastics are a global environmental problem and have been a cause for concern for many years. Although many reports have been written on the subject of microplastic and plastics the definitions used by medicine, science, industry etc are all slightly different although they share the fact that it is a solid material that can be molded and consists of polymers [Verschoor, 2015]. The International Organization for Standardization (ISO) defines plastic in ISO [2013] as "a material which contains as an essential ingredient a high polymer and which, at some stage in its processing into finished products, can be shaped by flow". Rubber meets this description, but are categorized differently by the ISO [ISO, 2013]. For the purpose of this report microplastics are categorized as: "Synthetic solid particles smaller than 5 mm, with a high polymer content. Persistent and insoluble in water" [Verschoor, 2015]. Non-degradeable

The main source of TRMP to the environment are abrasion from tires when driving on the road [Kole et al., 2017]. Particles are released due to the heat created while driving on the road and the shear forces between road and tire. Both heat and shear create particles. Shear forces result in relatively large particles, while the heat generated on the tire's surface causes volatile compounds to evaporate and release smaller particles [Kole et al., 2017]. The size distribution of the particles depend on factors such as temperature, pavement type, driving style, age and tire composition [Kole et al., 2017]. The size distribution of TRMP particles vary a lot in the literature, due to different sampling techniques, analytical equipment and the difficulties in seperating tire from road particles, since these usually form conglomerates with the tire particles [Grigoratos and Martini, 2014]. Grigoratos and Martini [2014] have looked at multiple studies focusing on the size distribution of tire wear and tear. Sizes range from 10 nm to 300 μm, with most particles being in the range of 50 to 100 μm. The density of tire rubber determines whether the particle will float or sink in water. The density of tire rubber is between 1.15 $\frac{g}{cm^3}$ and 1.18 $\frac{g}{cm^3}$ depending on the source [Banerjee et al., 2016; Dumne, 2013].

Kole et al. [2017] estimates that tire wear from all the worlds vehicles results in 5,917,518 tonnes of tire wear and tear annually. Although this is the largest source of TRMP to the environment tire rubber can also find its way into the environment from other sources. Between 1 and 1.5 billion waste tires are generated every year globally [Hamdi et al., 2021]. These end of life tires (ELT) are used in different processes in the civil engineering or energy sector. According to a press release from European Tyre and Rubber Manufacturers Association (ETRMA) 95% of the ELTs in the 32 member countries (EU27, Norway, Serbia, Switzerland, Turkey and UK) were collected and treated for material recovery and

energy recycling [ETRMA, 2021a]. 52% of the ELTs were recycled, this includes ELTs sent to granulation and the incorporation of the inorganic content of ELTs in cement manufacturing. 40% were used in energy recovery which includes being an alternative energy source for cement kilns and paper/pulp mills, thermal power staions, industrial boilers and pyrolosis, with 75% of that going to cement kilns as an energy source. 3% were used in civil engineering which includes retention basins and tire derived aggregates used in pavements. The remaining 5% are stocked, unknown or waiting for treatment [Hamdi et al., 2021; ETRMA, 2021a].

2.1.1 Pathways for tire rubber microplastic to the environment

Although ELTs are used in various applications such as rubber granules in synthetic turf fields [Marsili et al., 2014] or as rubber mulch in bioretention basins used in stormwater management [Kanematsu et al., 2009] the most abundant source of TRMP to the environment are still tire wear and tear from vehicles on roads [Kole et al., 2017].

TRMPs can find their way from the road to the environment through different pathways Kole et al. [2017] have made an overview of the different pathways for TRMP to the environment illustrated in figure 2.

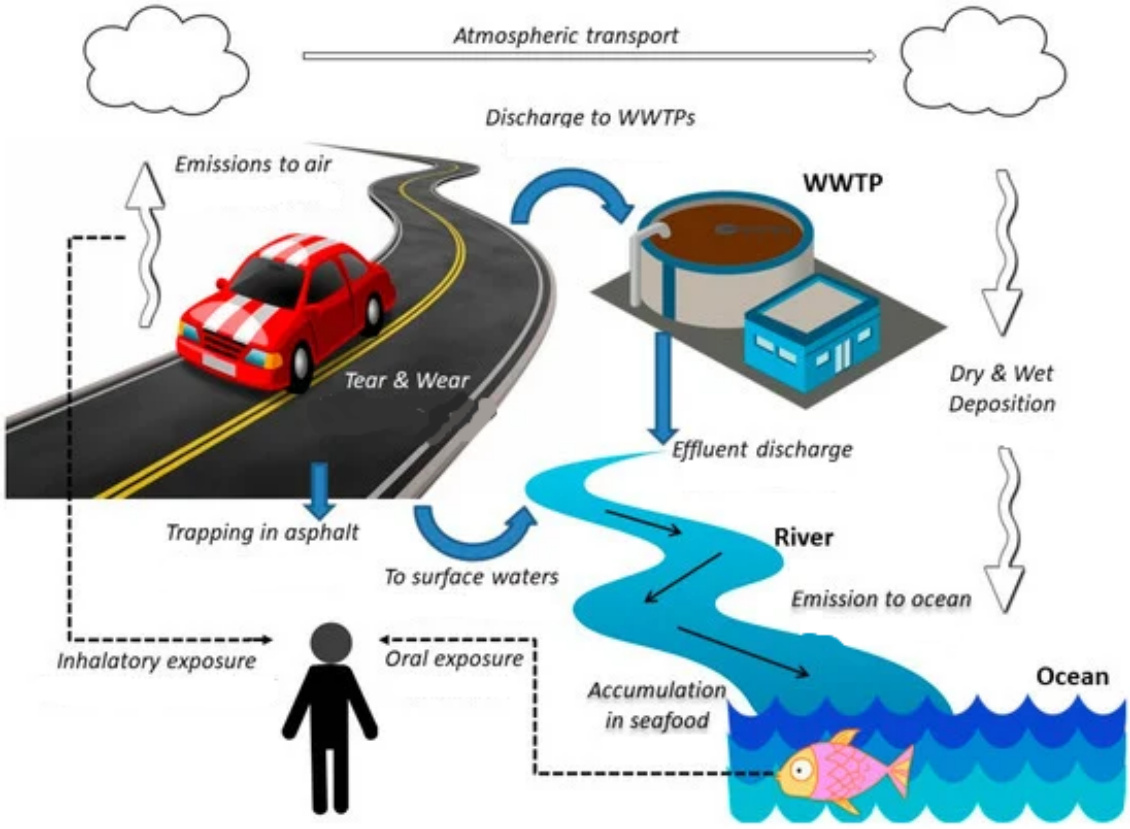

Figure 2. Pathways for tire wear and tear from the road into the environment. Figure from Kole et al. [2017].

The coarse fraction of the TRMP are deposited on the road surface. During rainfall events TRMP will be washed of the road. According to Unice et al. [2019] the rate of precipitation

should be at leat 2 mm/d for the particles to be mobilized and at 5 mm/d the majority of particles will be washed from the road some fraction of the particles will remain embedded in the road depending on the openness of the asphalt [Baensch-Baltruschat et al., 2020].

Depending on whether the road is in an urban or rural area or it is a highway the runoff rate to the aquatic environment will vary. Runoff directly to surface waters will be 10% of the TRMP outside of urban areas, while 90% will remain in the soil according to Broeke et al. [2008]. In urban areas 60% of the TRMP are released into the sewer system. In Denmark approximately 60% of the sewer system is separated, meaning that rainwater is led directly into the surface water. The remaining 40% are combined sewers leading the TRMP with the rainwater to a WWTP. Not many studies have been done with investigating only TRMP released from WWTP, but it can be assumed that the same percentage of MP particles that pass the WWTP will pass for TRMP. Studies from Sweden and Norway have shown that between 19.8% and 5.3% of microplastics in the size range >20 μm pass the WWTP while 0.6% of the MP with a size >300 μm pass through the WWTP and into the effluent [Magnusson and Wahlberg, 2014; Magnusson, 2014].

The smaller TRMP particles from the road will be dispersed through atmospheric transport. A recent study done by Evangeliou et al. [2020] modelled that 100,000 tonnes of tire wear particles are deposited through atmospheric transport to the world oceans. Kole et al. [2017] estimate that of the total TRMP that end up in the environment 67% end up in soil, 12% end up in air, 6% are emitted directly to surface waters and 15% enter sewers, 9% remain in the WWTP and the remaining the 6% pass through, making the total percentage that reach surface waters 12% [Kole et al., 2017]. This would indicate that of the 5,917,518 tonnes of TRMP emitted yearly calculated by Kole et al. [2017] 710.102 tonnes reach the aquatic environment. This doesn't take into consideration the amount of particles trapped in asphalt, which according to Kole et al. [2017] is 58% of total emissions making the total release to the aquatic environment 298.242 tonnes/year. With The Netherlands, which numbers Kole et al. [2017] are based on, having many roads with open asphalt for the particles to be trapped in. The actual release to the aquatic environment is probably in between these two numbers. Another unknown factor is the contribution from airborne TRMP. Although Evangeliou et al. [2020] have modelled the release of TRMP to the atmosphere the model does not consider photodegredation of TRMP in ambient air.

2.1.2 Fate of tire rubber microplastics in the environment

The breakdown of plastic in the environment usually happens through three major processes:

- Mechanical degradation
- Abiotic degradation
- Biotic degradation, [Zhang et al., 2021].

The general processes for the degradation of plastics can be seen in figure 3.

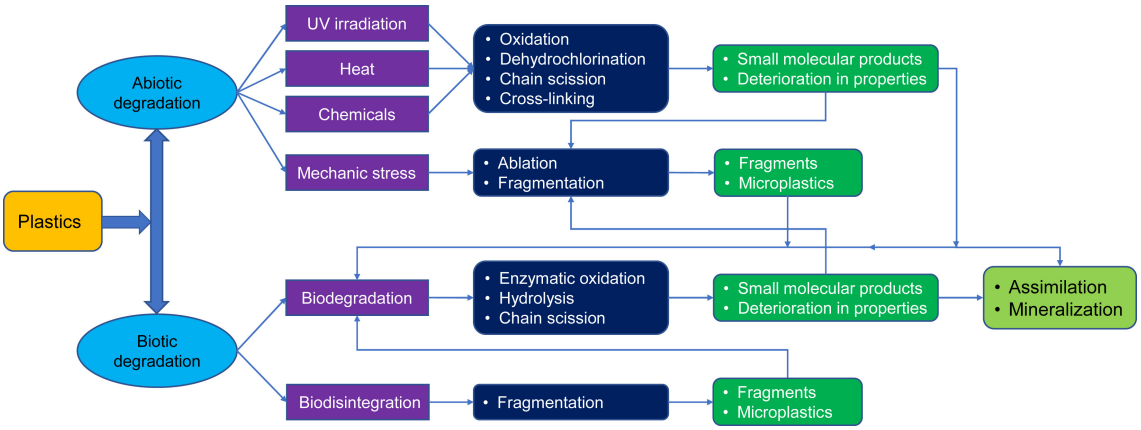

Figure 3. Schematic showing the general processes involved in the degradation of plastics in the environment. Schematic made by Zhang et al. [2021].

TRMP has already undergone mechanic stress before entering the environment due to the shear stress experienced on the road, therefore mechanic stress is not a huge factor on TRMP in the environment as it is on fx. larger macroplastics floating in the marine environment [Song et al., 2017]. However Song et al. [2017] showed that the combination of prolonged UV exposure together with mechanical abrasion of select MP particles degraded the plastic much more than only mechanical abrasion. Photodegradation by UV in the environment happens with UV light, with 95% in the range of 400-315 (UVA) and 5% in the range of 315-280 nm (UVB) [WHO, 2016]. Gewert et al. [2015] distinguish between two types of plastics in their analysis of polymers floating in the marine environment: Plastics with a carbon-carbon backbone and plastics with heteroatoms in the main chain. Natural rubber would fall under the first category since it contains monomers with unsaturated bonds that are susceptible to degradation by UV-light through the process of breaking the main polymer chain and creating a free radical [Gewert et al., 2015; Stevenson et al., 2008]. Synthetic rubber however are more dificult to categorize since it contains multiple crosslinks between the monomers consisting of mono-, di- and polysulphidic crosslinks as well as carbon - carbon bonds examplified in figure 4 [Holst et al., 1998].

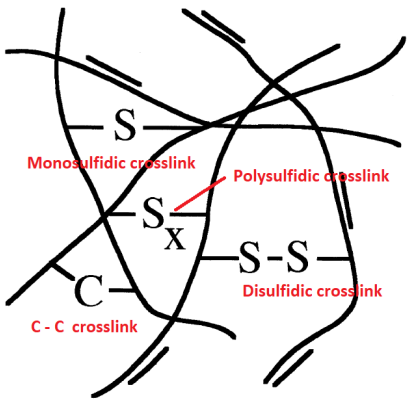

Figure 4. Example of the structure of vulcanized rubber with mono-, di- and polysulphidic crosslinks as well as C-C bonds binding the polyisoprene chains. Figure adapted from Holst et al. [1998].

The vulcanization process of tires makes them thermoset and generally very resistant to UV and thermal degradation [Halle et al., 2020].

Few studies have looked at the biological degradation of tire rubber and have focused primarily on the prevention of biological breakdown of tires [Holst et al., 1998]. Stevenson et al. [2008] suggests that rubber can be devulcanized and degraded by various fungal and prokaryotic organisms. Sulphuroxidizing bacteria such as *Thiobacillus spp.* can oxidize the disulfide links and thereby devulcanize the rubber making it easier to be broken down by thermal and UV degradation [Stevenson et al., 2008]. This is however still just in theory since tire rubber also contains compounds that inhibit biological growth such as zinc [Councell et al., 2004]. These compounds have to be removed before a biological degradation of tire rubber can be successful.

2.2 Toxic components in tire rubber

The ETRMA estimates that in 2019 alone 5 million tonnes of new tires were produced in the EU [ETRMA, 2021b]. The contents of a tire vary from manufacturer to manufacturer and also between the types of tires. An example of the contents ratio of a normal passenger tire can be seen in table 1

Table 1. An example of the material ratio in a standard passenger car tire. (From Continental [2014]

Material	**Percentage (Weight %)**
Rubber	41 %
Fillers	30 %
Reinforcing materials	15 %
Plasticizers	6 %
Vulcanizing chemicals	6 %
Anti-ageing agents and other chemicals	2 %

The rubber is typically a blend of natural and synthetic rubber. The natural rubber comes from the *Hevea* tree, while the synthetic rubber is derived from petroleum based products and is typically butyl rubber or styrene-butadiene copolymer [Martinez et al., 2013]. The fillers mostly consists of carbon black, an amorphous carbon structure used to strengthen and give abrasion resistance to the rubber, other fillers include clay, silica and calcium carbonate. Reinforcing materials are typically steel as well as synthetic fibers such as polyester, rayon or nylon [Continental, 2014]. Plasticizers are a mixture of aromatic, naphthenic and parrafinic oils used to soften the rubber to make it more workable. The vulcanizing chemicals consist of an organic sulphur compound (making the sulphur content in tire rubber around 1.5 %), stearic acid and ZnO. The sulphur compound is used together with an accelerator in the vulcanization of the tire while ZnO and stearic acid are used together as a catalyst for the process. In the vulcanization process a reaction happens between the accelerator, suplhur and the elastomers. Crosslinks are created between elastomers that results in high strenght and elasticity making the decomposition of the tire difficult [Martinez et al., 2013]. Despite the tire not decomposing easily, toxic components

still leach from tires and tire crumb rubber. Especially polycyclic aromatic hydrocarbons and zinc are toxic components of concern leaching from tire rubber [Capolupo et al., 2020; Lu et al., 2021; Unice et al., 2013; Wik, 2007]. According to Hartwell et al. [2000] the salinity of water has an effect on the toxicity of leachates from tire rubber. They found that toxicity of leachates decreases with increasing salinity up to salinity of 15 ppt. It is speculated that the reduced toxicity is due to a direct interaction between sea salts and the toxic leachates and that tire leachates pose a bigger threat to freshwater bodies than estuarine or marine habitats [Hartwell et al., 2000].

2.2.1 Polycyclic Aromatic Hydrocarbons

PAHs are organic compounds whose molecular structure consists of at least two or more fused benzene rings. PAHs stem from various sources as can be seen in figure 5, both natural and anthropogenic. Natural sources, such as volcanic eruptions and forest fires are not as significant as anhtropogenic emissions [Patel et al., 2020]. Incomplete combustion is one of the main sources of anthropogenic sources of PAH and includes activities like iron and steel production, refinery exhaust, power production, cement manufacturing, asphalt industries and rubber tire manufacturing [Patel et al., 2020].

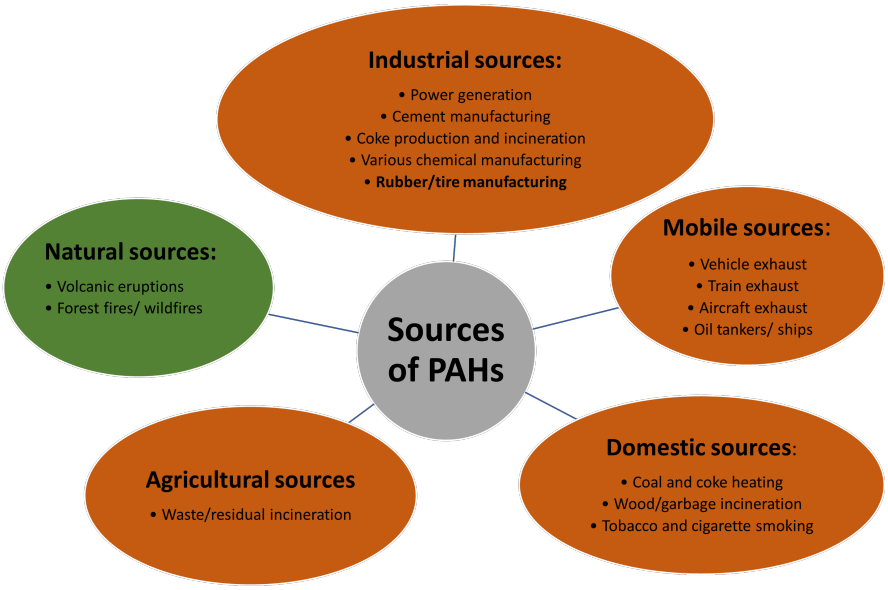

Figure 5. Different types of emission sources for PAHs. Red indicates anthropogenic emissions while green indicate natural emisions. Figure adapted from Patel et al. [2020].

A lot of PAH exists in the environment and therefore 16 of them are on the list of "priority pollutants" made by the USA-EPA. This list is used by many Environmental Protection Agencies around the world as a common practice for which PAH to analyse for in soil and water. These 16 PAH are often sorted by ring number when referenced in different studies [Keith, 2015]. The Danish EPA has evaluated the health risks and effects of PAH's released from tires [Nilsson et al., 2005]. They found that the investigated tires contained a row of different PAH's. Most abundantly the PAH's fluoranthene, pyrene, chrysene and the known carcinogenic benzo(a)pyrene (BaP) [Nilsson et al., 2005]. The following is an

overview of the 16 PAH, sorted by ring number with the amount found by Nilsson et al. [2005] in parentheses as average mg PAH per kg tire. The 16 PAH include:

2 rings

- Naphthalene, (Not detected).

3 rings

- Acenaphthylene, (Not detected).
- Acenaphthene, (Not detected)
- Anthracene, (Not detected)
- Fluorene, (Not detected)
- Phenanthrene, (Not detected)

4 rings

- Anthracene (Not detected)
- Benz(a)anthracene, (0.68 $\frac{mg}{kg}$)
- Chrysene, (5.48 $\frac{mg}{kg}$)
- Fluoranthene, (10.37 $\frac{mg}{kg}$)
- Pyrene, (25.7 $\frac{mg}{kg}$)

5 rings

- Benzo(a)pyrene (1.52 $\frac{mg}{kg}$)
- Benzo(b)fluoranthene (0.60 $\frac{mg}{kg}$)
- Benzo(k)fluoranthene (0.61 $\frac{mg}{kg}$)
- Dibenz(a,h)anthracene (0.35 $\frac{mg}{kg}$)

6 rings

- Benzo(ghi)perylene (6.83 $\frac{mg}{kg}$)
- Indeno(1,2,3-c,d)pyrene (1.07 $\frac{mg}{kg}$)

[Schmidt et al., 2015; Nilsson et al., 2005]

The carcinogenic properties of PAH depends on its structure and especially on the positioning of the aromatic rings in each molecule. The carcinogenic properties come from a biotransformation of the PAH via three enzymatic reactions that requires a bay structure of the aromatic rings in the PAH, exemplified in figure 6 with different relevant PAH's. The end product of these reactions is a vicinal dihydrodiol-epoxide that can react with the nucleophilic regions of the DNA [Diekman et al., 2019; Kim et al., 1997].

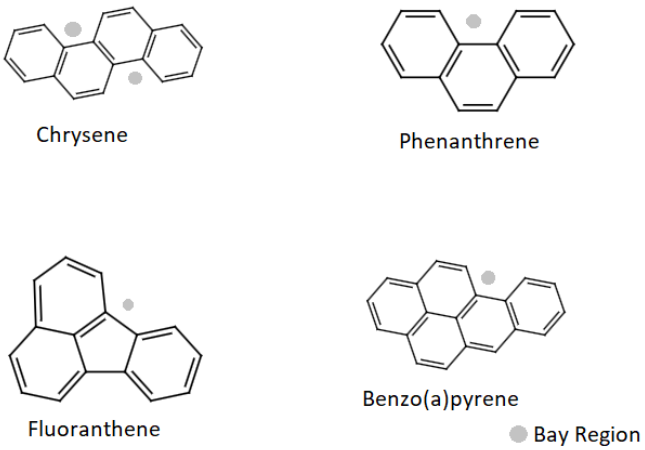

Figure 6. Chemical structures of selected PAHs, with bay region indicated.

The evaluation from the Danish Environmental Protection Agency found that the use of the discarded tires on playgrounds posed an insignificant health risk. The evaluation looked primarily at the effects of exposure through ingestion of sand and absorption through sweat. The content of PAH in the investigated tires varied between 11.4 mg/kg and 147.2 mg/kg [Nilsson et al., 2005].

Tang et al. [2018] have determined 16 PAHs in tire rubber samples using ultra-high performance supercritical fluid chromatography combined with atmospheric pressure photoionization-tandem mass spectrometry. From the 1 g of rubber sample they were able to detect 13 of the 16 PAH. The PAH with the highest concentration in the tire rubber was pyrene with a concentration of $24.31\frac{\mu g}{g}$ followed by fluoranthene with a concentration of $11.80\frac{\mu g}{g}$ [Tang et al., 2018]. They also investigated the PAH contents in other rubber types such as nitrile-butadiene rubber (NBR), ethylene-propylene-diene-monomer (EPDM) and natural rubber. The concentration of PAH in these rubber types were significantly lower than for those from tire rubber if at all detected [Tang et al., 2018].

Other studies have found PAH to leach from tires in the aquatic environment. The leaching of PAH from tires depend on many factors. Most notably the rubber formulation of the tire. Other factors include concentration of particles, alkalinity of the water and weathering of the particles [Wik, 2007]. PAH have been found to have photoinduced toxicity. Studies using *Daphnia magna* have found that the toxicity for various PAH increase when exposed to different types of UV light[Lampi et al., 2006; Wernersson and Dave, 1997]. One of the studies found that the toxicity to *D. magna* was increased 4.6, 5.5 and 178 fold for BaP, fluoranthene and pyrene respectively when exposed to UV light [Wernersson and Dave, 1997]. Another study also looked at 16 PAHs and 14 PAH photoproducts, also known as oxy-PAHs, toxicity to *D. magna*. The study found that the two most toxic compounds were photoproducts of BaP having EC50 values in the nanomolar range [Lampi et al., 2006].

As of 1 January 2010, the Registration, Evaluation, Authorisation and Restriction of

Chemicals (REACH), a regulating body under the European Parliament, has made a ban on the use, sale and import of extender oils containing certain PAHs for the use in tires and treads [REACH, 2009]. The oils may not exceed more than 1 $\frac{mg}{kg}$ of BaP or more than 10 $\frac{mg}{kg}$ for the sum of the following 8 PAH: Benzo(a)pyrene, benzo(e)pyrene, benzo(a)anthracene, chrysene, benzo(b)fluoroanthene, benzo(j)fluoroanthene, benzo(k)fluoroanthene and dibenzo(a,h)anthracene [REACH, 2009].

2.2.2 Zinc

Another potentially toxic compound leaching from tire rubber is zinc. Zinc occurs naturally in the environment and is an important trace metal. However in high concentration zinc can be toxic to aquatic organisms. Zinc is found naturally in the earths crust. It is released to the terrestrial and aquatic environment through, both natural and anthropogenic sources. However the anthropogenic sources are greater than those from natural sources [ATSDR, 2005]. The primary anthropogenic source of zinc to both air, water and soil come from mining and metallurgic processes, as well as the use of commercial products containing zinc. These products include fertilizers and wood preservatives [ATSDR, 2005]. Zinc concentrations in drinking water might be higher than the concentration found where the water was obtained due to leaching from galvanized pipes [ATSDR, 2005].

The Danish EPA (Miljøstyrelsen) has the following water quality standards for zinc: In freshwater 7.8$\frac{\mu g}{L}$, in soft freshwater (<24 mg $CaCO_3$/L) 3.1$\frac{\mu g}{L}$ and in saltwater 7.8$\frac{\mu g}{L}$. The maximum acceptable concentration is 8.4$\frac{\mu g}{L}$. These concentrations are to be added to the natural background level which in the North Sea is 1$\frac{\mu g}{L}$ [Miljøstyrelsen, 2016]. For drinking water the highest allowed concentration in the tap water is 3 $\frac{mg}{L}$ [Miljøstyrelsen, 2021].

Tire wear particles have been recognized for decades as a source of zinc to the environment [Dannis, 1974]. Tires contain approximately 1-2% by weight zinc [Councell et al., 2004; Rhodes et al., 2012]. Councell et al. [2004] have investigated the correlation between zinc concentrations in the sediment of different U.S. watersheds and annual daily traffic. They found a strong linear correlation between the two that can be seen in figure 7 [Councell et al., 2004].

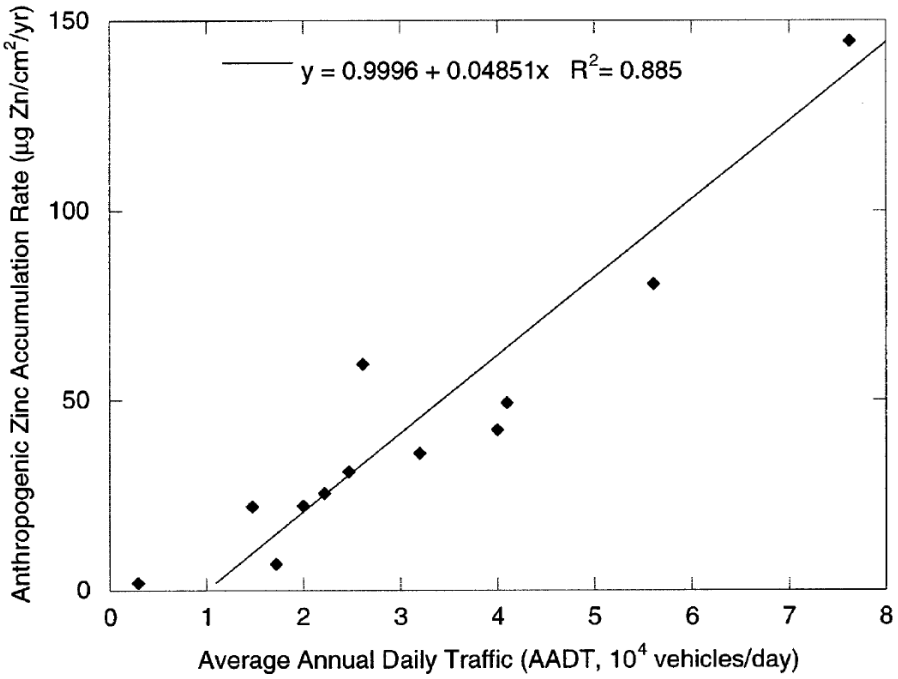

Figure 7. Correlation between average annual daily traffic and anthropogenic zinc accumulation rate. The graph is made by Councell et al. [2004] and uses data from sediment cores from 11 U.S. watersheds.

From figure 7 it can be seen that there is an apparent linear correlation between the average annual daily traffic and the anthropogenic zinc accumulation rate. Councell et al. [2004] saw this as evidence that tire wear is the main contributor of zinc to the environment from road traffic. The figure was compared with similar measurements of lead (Pb) that showed a decrease in sediment concentration around the 1980'ies when the use of lead in gasoline was in decline. A similar decrease was not seen for zinc and therefore the source of zinc to the sediment most be from tire wear [Councell et al., 2004].

The release of zinc from tire rubber in an aqueous environment are impacted by different factors. Dillon [2017] found a relation between the amount of zinc released from rubber mulch increased with decreasing temperatures. Since tires are created at high temperatures during the vulcanization process tires are more sturdy at higher temperatures and the breakdown of the tire rubber will therefore happen faster at lower temperatures [Dillon, 2017]. Another important factor in the release of zinc from tire rubber is the pH. A study by Kanematsu et al. [2009] investigating the risk of leachates from shredded rubber mulches, found that concentrations of zinc found in the simulated runoff water they used in their experiments contained higher concentrations of zinc at lower pH. Interestingly the study also investigated leaching at different temperatures and found that at pH 5 the concentration of zinc increased at increasing temperatures, while the concentration of zinc decreased at increasing temperatures at pH 9 [Kanematsu et al., 2009]. The study found the total concentration of zinc in the rubber mulch to be $4.89\frac{mg}{g}$ [Kanematsu et al., 2009]. The size of the rubber particles together with leaching time also affects the amount of zinc leached. Rhodes et al. [2012] found that the leaching of zinc from crumb rubber increased with decrease in crumb rubber size, and that the concentration of leachate

increased linearly over time in the investigated time period of 96 hours [Rhodes et al., 2012].

Wik et al. [2009] has investigated the effects of tire rubber leachates on different aquatic organisms, among these the algae *Raphidocelis subcapitata*, and found that the toxicity to the largest extend came from zinc and lipophilic organic compounds.

2.3 Effects of UVC and VUV treatment on plastics

UV treatment is becoming a very effective way of removing undesired microorganisms such as virus, bacteria and protozoa in wastewater as well as removing harmful substances in drinking water like pesticides or removing TOC from industrial wastewater [Hinjen et al., 2006; Yang et al., 2018; Zewde et al., 2020; Naderi et al., 2017]. According to Zewde et al. [2020] more than 20% of all WWTP in North America use UV as disinfection method. With UV disinfection becoming more and more used as a water treatment method it becomes relevant to also investigate what effects this treatment has on TRMP and its leachates. In wastewater treatment it is typically lamps that emit UV within the UVC range (200-280 nm) being used, since these wavelengths damage nucleic acids in the DNA and RNA of microorganisms, preventing the cell or virus from multiplying. The UV absorbance of DNA peak around 260 nm [Hinjen et al., 2006]. Experiments with pesticides performed by Yang et al. [2018] showed that Vacuum UV (100-200 nm) VUV/UV had a more significant effect than UV alone being more energy efficient and more efficient at removing pesticides from the water.

The main difference between UVC and VUV are that UVC is known to disrupt the bond in ozone (O_3) molecules while VUV will form O_3 . Peak O_3 generation happens at 185 nm, which is the wavelength of most comercial VUV lamps while peak O_3 degradation happens at 254 nm, which is the wavelength of most commercial UVC lamps [Claus, 2021]. Wavelengths shorter than 200 nm react with O_2 to form two free oxygen molecules that react with O_2 to form O_3. O_3 is very unstable and will break down naturally over time, but UV light with a wavelength of 240-315 nm will break the extra bond in O_3 and convert it back to O_2 [Claus, 2021]. It is this relationship that protects shorter wavelength UV from reaching the earths surface through interactions in the ozone layer.

In water VUV will form hydroxyl radicals through homolysis and photochemical ionization of water. The products of the homolysis are a hydroxyl radical and a hydrogen radical. The products of the photochemical ionization are a hydroxyl radical, a proton and a solvated electron. These products will take part in reduction and oxidation reactions in the water phase [Zoschke et al., 2014]. The photoinitiated oxidation of VUV can also remove organic matter from wastewater. Chen et al. [2021] have investigated the formation of nitrite (NO_2^-) and hydrogen peroxide (H_2O_2) when applying VUV irradiation to water. They measured the concentration of (NO_3^-), (NO_2^-) and (H_2O_2) in UVC and VUV/UV irradiated tap water and found that UVC irradiation increased (NO_2^-) formation while VUV/UVC increased (H_2O_2) formation [Chen et al., 2021]. In figure 8 the proposed pathways for the formation of (H_2O_2) and (NO_2^- are shown.

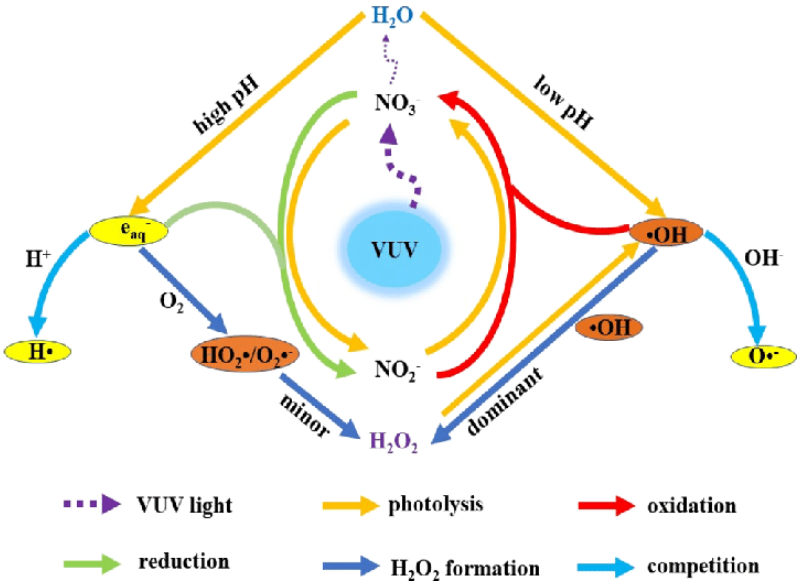

Figure 8. Proposed pathways for the formation of (H_2O_2) and (NO_2^-) in UV/VUV irradiation. Schematic made by Chen et al. [2021].

Both UV at naturally occurring wavelengths as well as UVC and VUV have been shown to degrade the surface of microplastics and cause the release of additives and chemical residues from the plastics [Lin et al., 2020; Sørensen et al., 2021]. Lin et al. [2020] showed that very high doses of UVC and VUV irradiation caused a significant alteration of the chemical features, surface morphology and hydrophobicity of the microplastics. Suggesting that the irradiation would have an effect on the adsorption of organic cotaminants. The degradation is attributed to the OH radicals created by VUV photolysis with H_2O [Lin et al., 2020]. UV is also known to create many other reactive oxygen radicals in water [Jager et al., 2017]. VUV have even been shown to create H_2O_2 in water with dissolved oxygen [Du et al., 2021].

Cataldo et al. [2010] have investigated the effects that O_3 have on the surface oxidation of tire rubber crumb. The study found that the ozonization releases CO_2 from the rubber and that the process is limited to the surface of the rubber and does not affect the bulk properties [Cataldo et al., 2010]. It is expected that intense UV and VUV radiation will have similar effects on TRMP as it has been shown to have on other MP.

Rosinska [2021] has looked at the effects of UV radiation from a UV low pressure lamp (254 nm) with a dose of 15–50 mW s/cm2 on the 16 EPA PAHs in treated wastewater. The study found that UV radiation had a positive effect on the removal of PAH and that. During the optimal exposure time of 30 min the total amount of PAHs decreased by 66%. The study also found that the higher the PAHs with a lower ring number had a higher removal rate with the UVC [Rosinska, 2021].

There are no known effects of VUV or UVC on zinc, although Burleigh et al. [2003] found zinc to be the metal most affected by photo-corrosion when exposed to UV light.

3 Materials and Methods

3.1 Treatment of tire rubber micro plastic with UVC

Tire rubber micro plastic (TRMP) were provided by the company Genan (Viborg, Denmark). The specific particles used were GENAN 120 Mesh (Genan). The particles had a size of <125 µm. The size fraction was obtained by sieving the particles through an Air Jet sieve 200 LS (Hosokawa Alpine). The sieve analysis was performed by Genan [GENAN, 2022]. The particles were suspended in tap water in glass petri dishes in concentrations of 1 g/L. An example can be seen in figure 9.

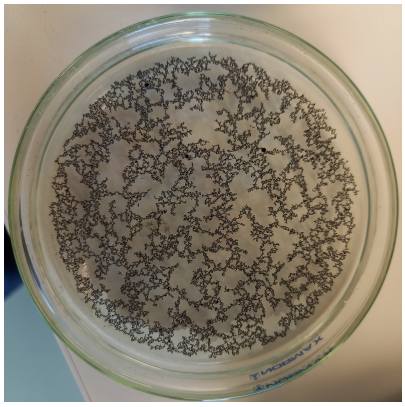

Figure 9. An image of the glass petri dish containing the suspended particles in tap water.

The setup for the treatment with UVC can be seen in figure 10. The samples were exposed to different duration of UVC light under a UVP 3UV lamp (Analytik Jena) placed 12 cm above the petri dish. The intensity of the lamp was measured just above the water surface at $650\frac{\mu W}{cm^2}$ with a SDL470 UVC light meter (Extech). The solution in the petri dish were stirred with a magnet stirrer. All samples were suspended in water for 2 hours regardless of the duration of UV exposure to ensure the same suspension time for all samples. When the sample had reached the desired amount of UVC the lamp was turned off and the sample was left on the stirrer for the remaining time of the 2 hours. After exposure the samples were transfered to 15 mL centrifuge tubes (VWR) which were centrifuged at 1000 RPM for 10 minutes in a ScanSpeed 1236R centrifuge (LaboGene) in order to separate the supernatant and the particles. The supernatant was extracted and used for toxicity test immediately after being centrifuged.

3.1.1 Alternative method

After conducting the first experiments a faster method were developed to accumulate more replicates faster. The setup is similar to the one described above and shown in 10. However

instead of only extracting the supernatant at the end of the 2 hours the UV lamp was left on for the entire duration of the 2 hours and samples were extracted continuously after the desired amount of UVC exposure. The concentration was kept the same and the extracted samples were kept at room temperature until the last sample were extracted after 2 hours. The samples were then centrifuged for 10 minutes at 1000 RPM and used for toxicity test immediately after being centrifuged. After analysing the data for this method it was found that there were a too high variance in the results, as well as the results differing too much from what was found with the original method. The advantages gained from being able to treat more samples faster were deemed too small, compared to the loss of both accuracy and precision in the results. The method was ultimately not used in the further experiments.

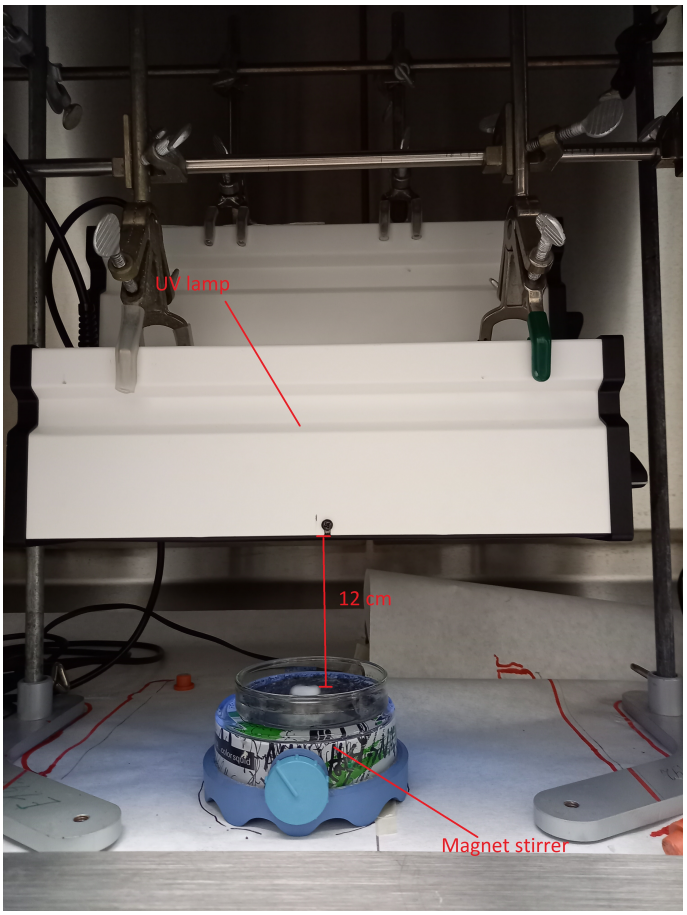

Figure 10. A picture showing the setup of the UVC treatment of the TRMP.

3.2 Treatment of tire rubber micro plastic with VUV+UVC collimated beam

TRMP particles were suspended in tap water for treatment with VUV+UVC light similarly as had been done for UVC treatment. Using the same concentration (1 g/L) and the same particle size (<125 µm). See the example shown in figure 9.

The setup for the VUV+UVC were provided by UltraAqua (Aalborg, Denmark). The

collimated beam setup can be seen in figure 11, with a description of the individual parts.

The VUV+UVC setup is flushed with 0.2 bar N_2 gas for 15 minutes, before turning on the VUV+UVC lamp. The VUV+UVC lamp is a Strahler NIQ 40/18 low pressure VUV lamp (Heraeus) see appendix 1. The lamp is given 5 minutes to heat up. The cooling water is turned on and cycled through a HTS 15 heat transfer station (Huber) set to 18 °C. The TRMP sample in the petri dish is placed on the magnet stirrer in the sample holder. The scissor lift is extended until resistance is felt indicating that the sample holder closes tight and the edge of the petri dish touches the lens of the tube. This is done in order to ensure no O_2 between the sample and the output of the lamp. O_2 in the system could lead to the creation of O_3 through photolysis. This is not desirable since O_3 in the system could block some of the UV light and lower the radiation output. The shutter is opened and the sample is exposed for the desired amount of time. The UVC output from the lamp was measured with a SDL470 UVC light meter (Extech) to be $120\frac{\mu W}{cm^2}$ at 254 nm. The output at 185 nm and at 254 nm was also measured by UltraAqua and the fluence was calculated based on water depth in the petri dish, reflection factor and water factor to be $120\frac{\mu W}{cm^2}$ for 254 nm and $13\frac{\mu W}{cm^2}$ for 185 nm. This makes the total fluence of UV $133\frac{\mu W}{cm^2}$ VUV+UVC, with 10 % coming from the 185 nm fraction. The technical data sheet for the lamp can be seen in appendix 1. This lamp had a lower output than the one used for only UVC irradiation and therefore it was necessary to have the samples exposed for longer periods with the maximum exposure time being 8,3 hours. After exposure the samples were transfered to 15 mL centrifuge tubes (VWR) which were centrifuged at 1000 RPM for 10 minutes in a ScanSpeed 1236R centrifuge (LaboGene) in order to separate the supernatant and the particles. The supernatant was extracted and used for toxicity test immediately after being centrifuged.

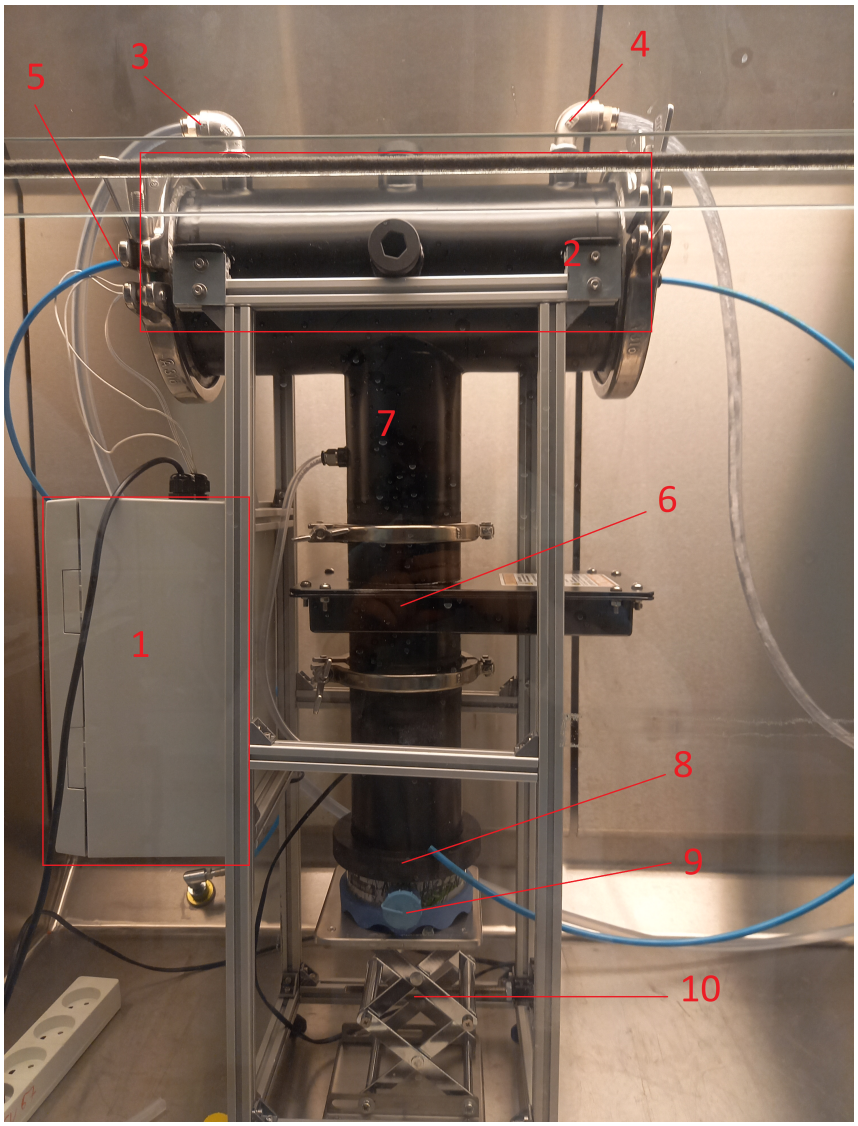

Figure 11. Setup for VUV+UVC treatment: 1) Power for VUV+UVC lamp. 2) Cooling-water filled chamber containing VUV+UVC lamp. 3) Inflow for cooling. water. 4) Outflow for cooling water 5) Inflow for N_2 gas. 6) Shutter allowing for VUV+UVC light to pas or to block of the light from the sample. 7) N_2 filled tube directing the collimated beam from the VUV+UVC lamp to the sample. 8) A sample holder. It holds the petri dish in place on the magnet stirrer and allows for minimum amount of O_2 to enter. 9) Magnet stirrer. 10) Scissor lift. Used to adjust the height of the sample so that the top of the petri dish touches the lens of the tube.

3.3 UVC and VUV effects on supernatant from a TRMP solution

After analysing data from the toxicology tests with UVC and VUV+UVC treated TRMP effects on *R. subcapitata* it was clear that analysing the effects of UVC and VUV on only the leachates of TRMP were important to understand the full effects of UVC and VUV treatment. An experiment was set up were 1.00 g of the TRMP were added to a 1 L bluecap bottle and filled up with 1 liter of tap water, making the concentration of TRMP in the bottle 1g/L. The solution was left in the bluecap bottle, in a climate room at 10 °C on a magnet stirrer for 21 days. After the 21 days the solution was pipetted into 50

mL greiner centrifuge tubes (Sarstedt) and centrifuged in a ScanSpeed 1236R centrifuge (LaboGene). The supernatant was then extracted and filtered into a clean 1 L bluecap bottle through a GF-75 glass fiber filter paper (Advantec) with a size of 47 mm and a pore size of 0.3 μm to ensure that no TRMP particles were left in the supernatant. The supernatant was stored in a dark climate room at 10 °C in a 1 L bluecap bottle until it was used for further experiments. The supernatant was treated with UVC and VUV+UVC for the same duration and intensity as described for solutions containing TRMP particles and toxicology tests were made with the *R. subcapitata* algae. It was necessary to dilute the control test for the 21 day supernatant in 1:3 algal growth medium, before going through the procedure of the algal test, since initial tests showed a too high toxicity to make a proper non-linear fit.

3.4 Toxicity of UV treated TRMP and supernatant measured as growth inhibition of *Raphidocelis subcapitata*

To test the toxicity of the supernatant from the micro plastic solutions a growth inhibition test was conducted in accordance with ISO standard 8692:2012 [ISO, 2012]. Algea cultures of *R. subcapita* were grown for 2-5 days in climate chamber at 20 C°. A 96 clear well microplate was prepared with a mix of algal growth medium and the supernatant from the UVC treatment of the TRMP. Having a control column containing only algal cells and growth medium and a blank column containing only growth medium. The rest of the columns contain different concentrations of the supernatant from the original solution of 1000 mg/L TRMP that has been diluted 2 fold between each well. The different concentrations in the microplate wells can be seen in table 2.

Table 2. The concentrations of supernatant in the different well columns in the algal growth plate. The concentrations are based on the original solution of 1000 mg/L TRMP solution.

Control	1 $\frac{mg}{L}$	2 $\frac{mg}{L}$	3.9 $\frac{mg}{L}$	7.8 $\frac{mg}{L}$	15.6 $\frac{mg}{L}$	31.3 $\frac{mg}{L}$	62.5 $\frac{mg}{L}$	125 $\frac{mg}{L}$	250 $\frac{mg}{L}$	500 $\frac{mg}{L}$	Blank

The microplate was placed under a lamp panel for plant growth giving 8000 lux of light for 72 hours. After 72 hours the biomass in the microplate was measured with a Thermo Multiskan Plate Reader at 450 nm. A picture of the microplate after 72 hours can be seen in figure 12. The growth results from the microplate was then used to create growth inhibition curves in order to find a EC50 value.

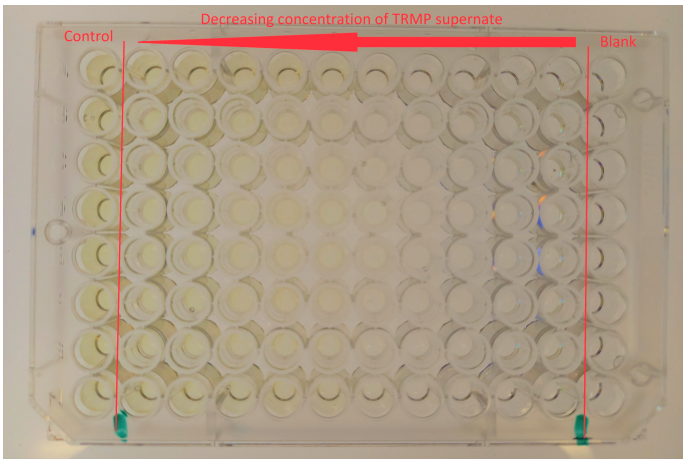

Figure 12. An example of an algal growth plate with *R. subcapitata* after 72 hours of growth. The right most column only contains growth medium, while the left most only contains growth medium and algal cells, but no supernatant. The middle rows contain algal cells, growth medium and supernatant diluted 2 fold from right to left.

3.5 Zinc quantification with photometric zinc test

To quantify the content of zinc in the samples a Speqtroquant photometric zinc test 1.14832 (Merck) was used. The test kit is used for water samples containing zinc and can be used in the range of 0.05 - 2.50 $\frac{mg}{L}$ Zn. Due to the fact that the test kit is designed to be used with the speqtroquant (Merck) type of spectrophotometers it was necessary to first make a standard curve for the correlation between zinc concentration and absorbance. For the standard and subsequent zinc quantification tests a Genesys 20 spectrophotometer was used. The spectrophotometer was set to a wavelength of 565 nm in accordance with Supelco [2021]. The spectrophotometer was calibrated against a sample with distilled water and the reagents from the test kit. An example of the calibration sample and a sample containing zinc can be seen in figure 13.

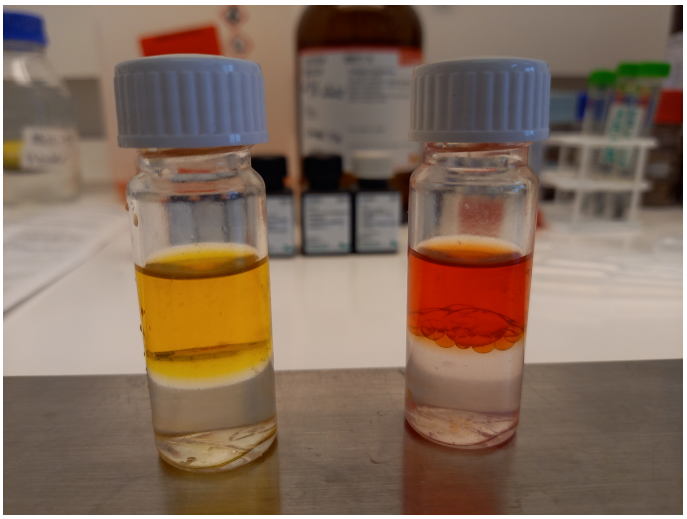

Figure 13. Example of the zinc test tubes containing the organic phase (Isobutyl methyl ketone) with the colorant (pyridylazonaphthol derivative) and the zinc extract before extraction to 10 mm cell. To the left is an example of a blank test with distilled water. On the right is an example of a test containing zinc.

To make the standard curve for the zinc test 600 mg of $ZnCl_2$ is weighed of and dissolved into 50 mL of distilled water. 2 mL of this solution is transferred to a 100 mL beaker and further diluted with 100 mL of distilled water. 20, 50, 100, 150 and 200 µl are extracted from the 100 mL zinc solution and transferred to 15 mL test tubes where 10 mL of distilled water is added to obtain the final solutions within the detection range of the zinc test kit. For both the standard curve and the samples of the treated and non-treated TRMP supernatant 5 mL of the sample is added to the test tubes. Four reagents (sodium hydroxide, N,N-dimethylformamide, formaldehyde, methanol and potassium cyanide) from the test kit are added and the tube is shaken and left to react for 3 minutes. The zinc ions react with a pyridylazonaphttol derivative to form a red complex as seen in figure 13 right. The fifth reagent (Sodiumdiethyldithicarbamate trihydrate) is added and dissolved by shaking the tube vigorously. 5 mL of Isobutyl methyl ketone (organic phase) is added and the tube is shaken vigorously for 30 seconds before being left to stand for 2 minutes until the organic phase has separated (see figure 13). The organic phase (upper phase) is withdrawn with a suction pipette and transferred to a 10 mm cuvette (Sarstedt). The cuvette is put in the spectrophotometer and the absorbance at 565 nm are read. The obtained standard curve used for conversion from absorbance to zinc concentration can be seen in figure 14.

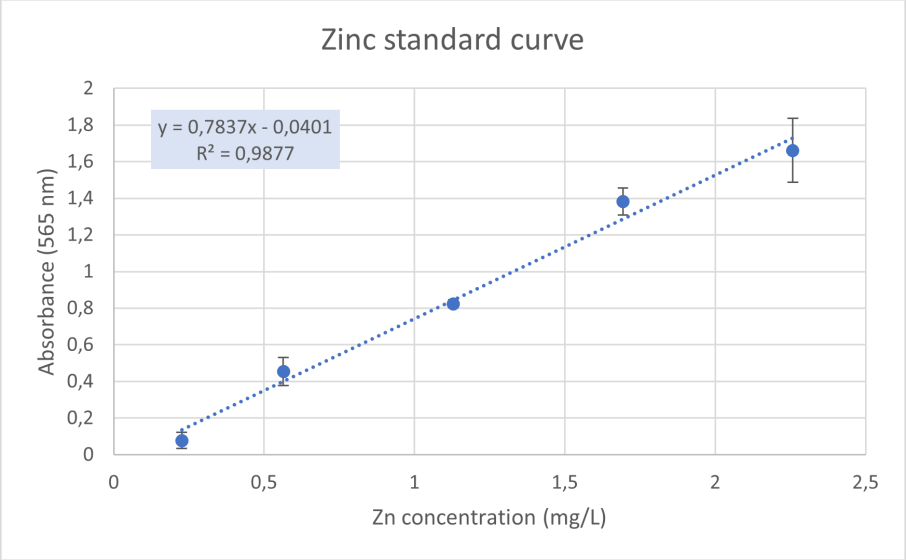

Figure 14. Standard curve for the relationship between zinc concentration and absorbance at 565 nm. Each concentration was measured 3 times and variations are shown on the graph.

3.6 PAH quantification with Gas Chromatography

In order to quantify PAH in all samples, both those treated with UVC and VUV+UVC and those not treated it was necessary to select certain PAHs since it wasn't possible to quantify all PAHs within the scope of this project. Three PAH were selected based on the following criteria: Availability, high content in tire rubber and carcinogenic properties. The three PAH selected were pyrene, fluoranthene and benzo(a)pyrene. Pyrene and fluoranthene were selected due to them being the most abundant PAHs in tire crumb rubber, as found by both Diekman et al. [2019] and Marsili et al. [2014]. Benzo(a)pyrene was selected due

to it being a known carcinogen and being a good indicator for other carcinogenic PAHs. For the quantification of PAHs in the water samples a method was developed based on the method used by Polyakova et al. [2013] to determine PAH in water by gas chromatography with flame ionization (GC-FID). An Agilent 7890A Gas Chromatograph (USA) equipped with a Combi PAL autosampler was used for the quantification of PAHs. The column temperature was programmed as follows: Initial temperature 150 °C (1 min) then a rate of 15 $\frac{^{\circ}C}{min}$ up to 260 $^{\circ}C$ the temperature is then held at 260 $^{\circ}C$ for 6 minutes. 1 μL of the sample is injected into the injector and blown through with helium as a carrier gas at a speed of 2.3 $\frac{mL}{min}$. All results were processed with Agilent Chem Station software. Fluoranthene has a retention time of 396 seconds, pyrene has a retention time of 420 seconds and BaP has a retention time of 738 seconds. Firstly three stock solutions were made one by adding 1000 mg of pyrene to 10 mL of distilled water, one by adding 500 mg of fluoranthene to 10 mL of distilled water and one by adding 100 mg BaP to 10 mL in a 14 mL glass serum bottle. The serum flasks were centrifuged for 5 minutes at 4000 rpm in a ScanSpeed 1236R centrifuge (LaboGene) to dissolve the PAHs. 200 µl, 150 µl, 100 µl, 50 µl and 20 µl from each stock solution were added to a 9,5 mL glass serum flask and diluted with 5 mL of distilled water. These solutions were used to make a standard curve for the gas chromatography. The standard curve can be seen in figure 15.

The solutions used for the standard curve and the water samples from the TRMP supernatant were prepared for the GC-FID in the same way. The 2 mL of the water sample was added to a 9,5 mL sterilised glass serum bottle. 1.5 g of Na_2SO_4 is added gradually while the sample is shaken. 2 mL of a toluene-hexane solution (1:6) is added to the serum bottle and the sample is centrifuged for 5 minutes at 4000 rpm in a ScanSpeed 1236R centrifuge (LaboGene). The toluene-hexane (1:6) is extracted from the serum bottles and added to GC vials and analysed with the gas chromatograph.

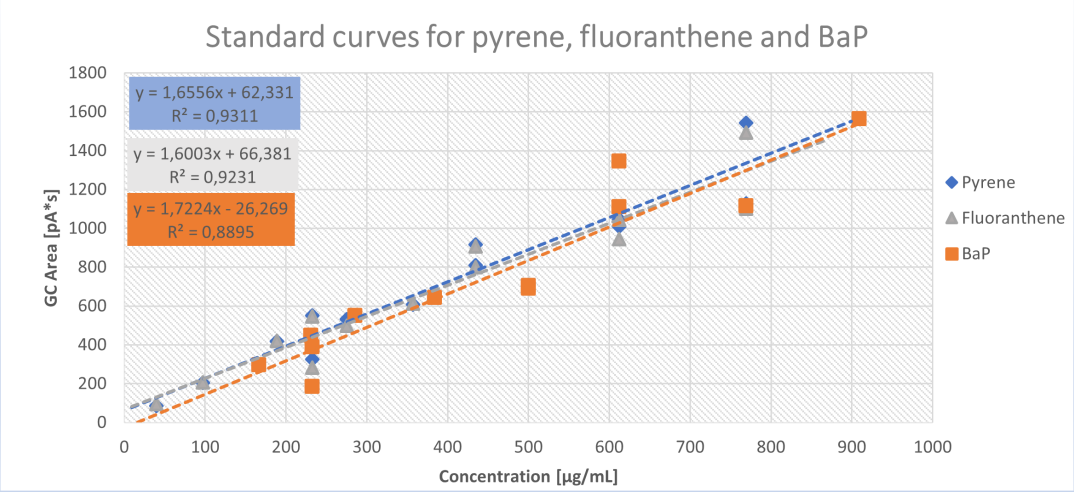

Figure 15. Standard curve for the relationship between concentrations of pyrene, fluoranthene and BaP in relation to the area under the individual peaks for the respective PAHs

3.7 Fitting of growth inhibition data to different non-linear models

The data from the algal growth in the microplates where plotted with inhibition of growth against concentration of TRMP in mg/L. They were fitted against two different non-linear models in the mathematical software program Maple. Model 1 was a logistic model of the equation:

$$y = \frac{1}{1 + \exp^{-(\alpha+\beta \cdot log(x))}} \tag{3.1}$$

Where x is the concentration of TRMP in mg/L, y is the inhibition ranging from 0 to 1 and α and β are model parameters.

Model 2 was based on the Langmuir-Hill model and of the formula:

$$y = \frac{x}{x + a} \tag{3.2}$$

With x being the concentration of TRMP in g/L, y being the inhibition ranging from 0 to 1 and a being a model parameter. Two models were used both to see if one model was better than the other, but also to visually analyse the goodness of fit to the data and the overall usability of the inhibition data from the toxicology experiments with *R. subcapitata*. The two models were chosen since they both are used to express effect from a compound to an organism. An example of one of these fits can be seen in figure 16. It was found that, both models made good fits. All data have been fitted to both models. All EC50 values mentioned in the results have been found by using model 1.

3.7.1 Statistical significance of data

The EC50 values from the different treatments were compared using a Wilcoxon rank-sum test in order to asses whether the data could be considered coming from different populations. The Wilcoxon rank-sum test was conducted in Excel using a statistical analysis tool.

4 Results

4.1 Toxicity of UVC treated TRMP

In figure 16, there is an example of how all the data was analyzed and fitted to the two non-linear models. Both models fit the data, but model 1 is the model that was used to further analyze the data. The fit seen in figure 16 are for the inhibition data from UVC treatment with 2.75 $\frac{J}{cm^2}$ UVC. For a full overview of the different inhibition curves see appendix 2.

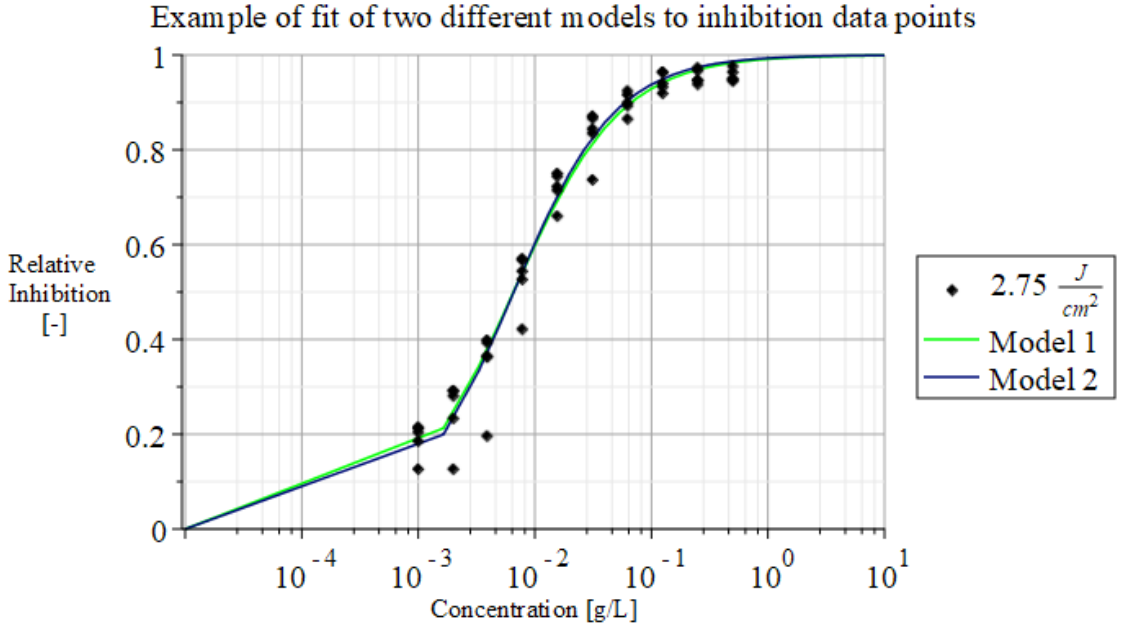

Figure 16. An example of the fit made with models 1 and 2 to the growth inhibition data.

Figure 17 shows all growth inhibition curves from different treatments with UVC. In the figure is the inhibition curve from the control samples and samples treated with 0.25 $\frac{J}{cm^2}$ UVC, 1.5$\frac{J}{cm^2}$ UVC, 2.75$\frac{J}{cm^2}$ UVC and 4.5$\frac{J}{cm^2}$ UVC respectively. All data points are plotted alongside the inhibition curves. There is a shift towards the left for the curves that indicate higher toxicity for some of the UVC treatments. The curves are made from 6 replicates consisting of 6 independent experiments for each treatment. The control is also made from 6 replicates.

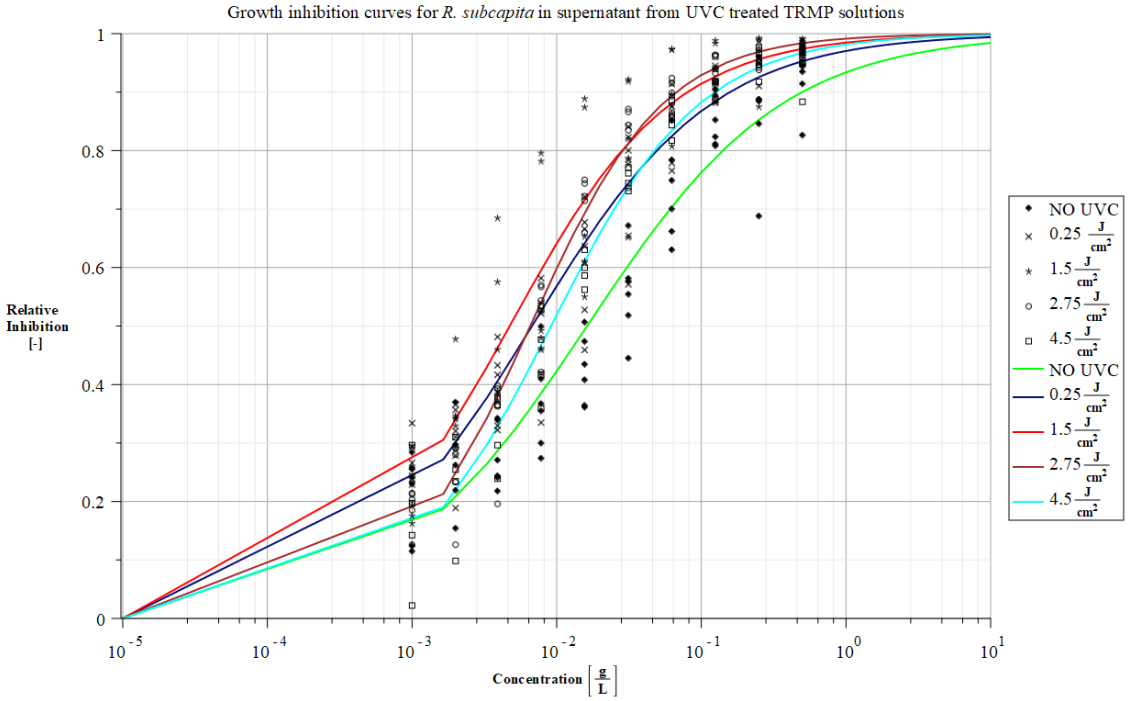

Figure 17. Growth inhibiton curves from all treatments with different intensities of UVC. The data points come from 6 different experiments of the same intensity made for all 4 intensities of UVC and the control.

From the growth inhibition curves in figure 17 EC50 values were obtained for the different treatments. The results of this can be seen in figure 18.

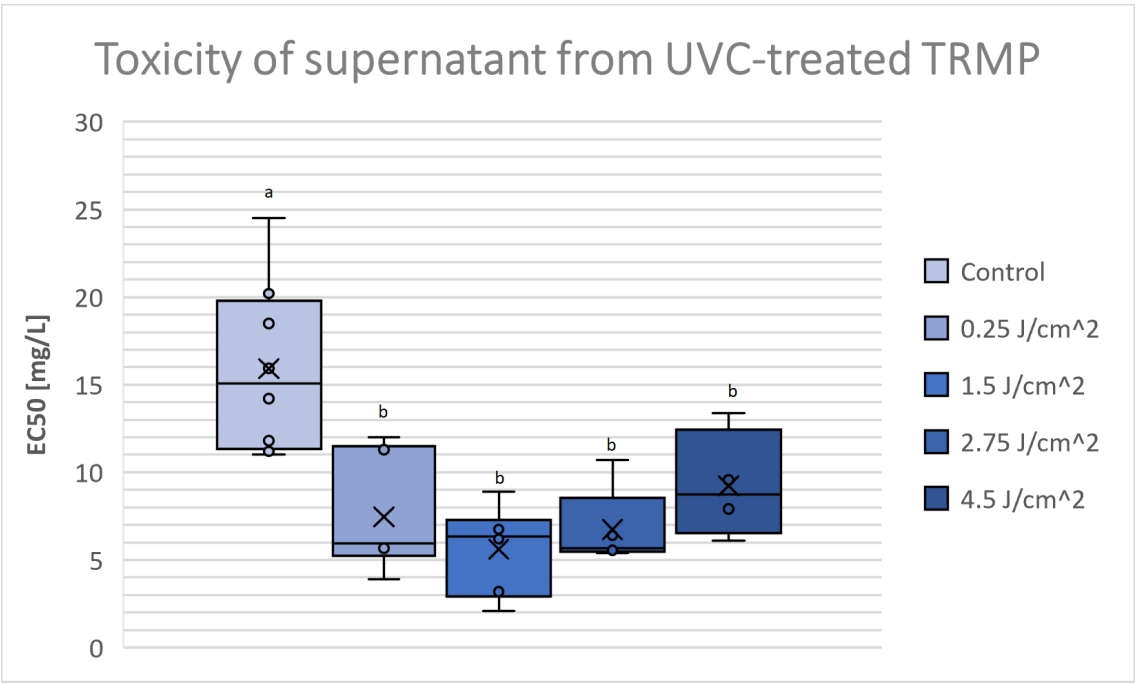

Figure 18. Boxplots showing EC50 from the control and different treatment intensities representing the toxicity of the supernatant from UVC treated TRMP. The boxplots have been assigned a letter depending on whether they are significantly different from each other with a P-value of <0.05.

The control has an average EC50 value of $15.92 \pm 4.54 \frac{mg}{L}$, while the samples treated with 0.25 $\frac{J}{cm^2}$ UVC, $1.5 \frac{J}{cm^2}$ UVC, $2.75 \frac{J}{cm^2}$ UVC and $4.5 \frac{J}{cm^2}$ UVC have average EC50 values of $7.46 \pm 3.05 \frac{mg}{L}$, $5.61 \pm 2.29 \frac{mg}{L}$, $6.74 \pm 2.01 \frac{mg}{L}$, and $9.24 \pm 2.69 \frac{mg}{L}$ respectively.

In order to figure out if there is any statistically significant difference between the non-UV treated supernatant, and the supernatant treated at different UVC intensities, a wilcoxon rank sum test was conducted. The results can be seen in table 3.

Table 3. P- values from wilcoxon rank sum test for the comparison of EC50 values between the different treatment intensities and no treatment with UVC. P<0.05 is marked with (*) and P<0.01 is marked with (**).

	Control	**0.25** $\frac{J}{cm^2}$	**1.5** $\frac{J}{cm^2}$	**2.75** $\frac{J}{cm^2}$
0.25 $\frac{J}{cm^2}$	0.014*	-		
1.5 $\frac{J}{cm^2}$	0.0020**	0.69	-	
2.75 $\frac{J}{cm^2}$	0.0034**	0.47	1	-
4.5 $\frac{J}{cm^2}$	0.027*	0.29	0.14	0.14

Table 3 shows that there is a significant difference between the EC50 values of the control and the TRMP treated with UVC, but not any significant difference between the treatments with different intensities of UVC.

Figure 19 shows the concentration of zinc released from TRMP treated with different doses of UVC and the non-treated control. The figure shows the concentration of Zn in $\frac{mg}{L}$, which is equivalent to mg zinc released per g of TRMP, since the solution of TRMP in tap water used is 1 $\frac{g}{L}$.

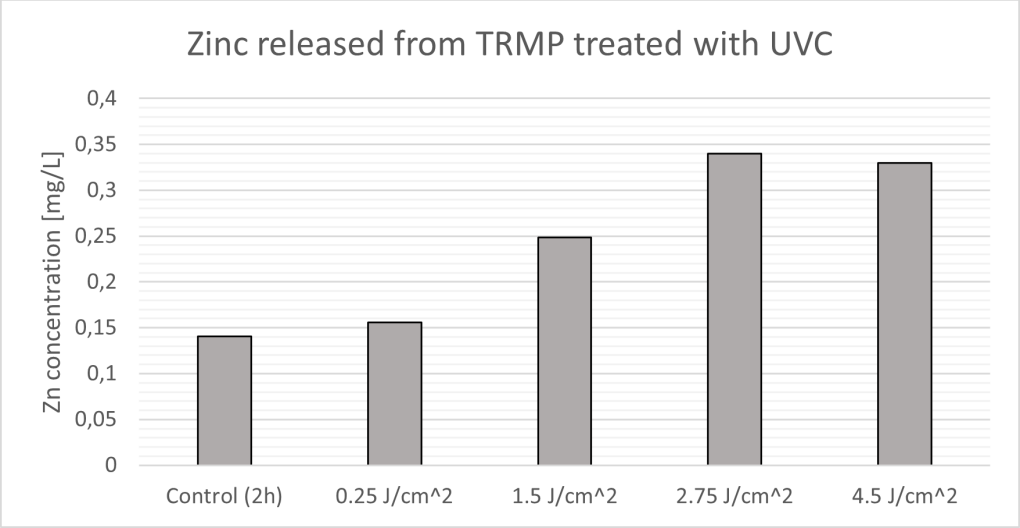

Figure 19. Zinc concentration in TRMP solutions treated with different doses of UVC. Determined with the photometric zinc test.

As seen from figure 19 the lowest measured zinc concentration was found in the control ($0.14 \frac{mg}{L}$ Zn), while the highest concentration was measured in the TRMP treated with $2.75 \frac{J}{cm^2}$ ($0.34 \frac{mg}{L}$ Zn) and 4.5 $\frac{J}{cm^2}$ UVC ($0.33 \frac{mg}{L}$ Zn). Overall there is an increase in release of zinc from the TRMP when exposed to increasing doses of UVC.

Figure 20 shows the release of the three PAHs fluoranthene, pyrene and BaP from TRMP solutions treated with UVC at different doses.

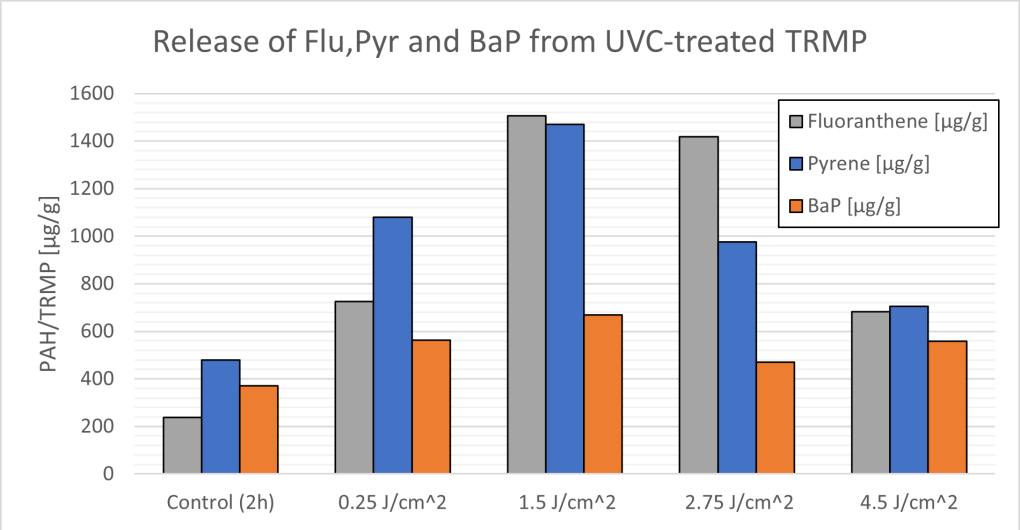

Figure 20. The release of fluoranthene, pyrene and BaP in TRMP solutions treated with different doses of UVC. Expressed in μg PAH per g of TRMP.

Figure 20 shows an increase in release of PAH from the TRMP when exposed to increasing UVC doses to $1.5\frac{J}{cm^2}$. UVC doses of $4.5\frac{J}{cm^2}$ appears to decrease fluoranthene and pyrene relative to $1.5\frac{J}{cm^2}$.

4.2 Toxicity of VUV+UVC treated TRMP

Figure 21 shows all growth inhibition curves from different treatments with UVC. In the figure is the inhibition curve from the control samples and samples treated with 0.25 $\frac{J}{cm^2}$, 0.5 $\frac{J}{cm^2}$, 1.0 $\frac{J}{cm^2}$, $1.5\frac{J}{cm^2}$, $2.75\frac{J}{cm^2}$ and $4.5\frac{J}{cm^2}$ VUV+UVC respectively. All data points are plotted alongside the inhibition curves. There is a shift towards the left for the curves from the control with no treatment that indicate higher toxicity for some of the VUV+UVC treatments. The curves are made from 6 replicates consisting of 6 independent experiments each treatment. The control is also made from 6 replicates.

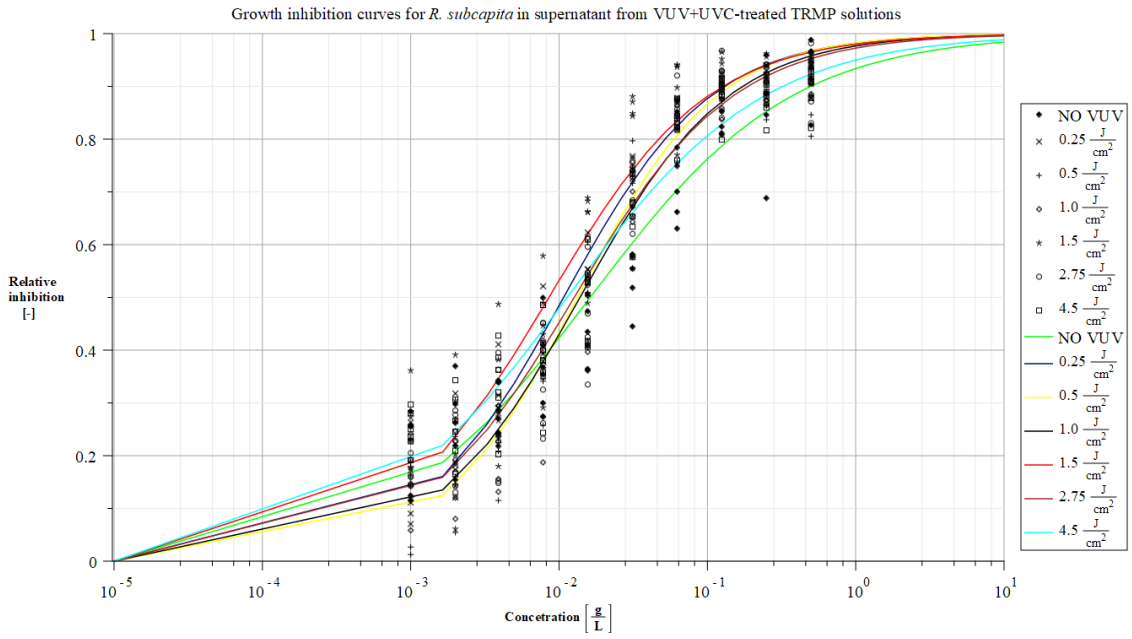

Figure 21. Growth inhibiton curves from all treatments with different intensities of VUV+UVC.

From the growth inhibition curves in figure 21 EC50 values were obtained for the different treatments. The results of this can be seen in figure 22.

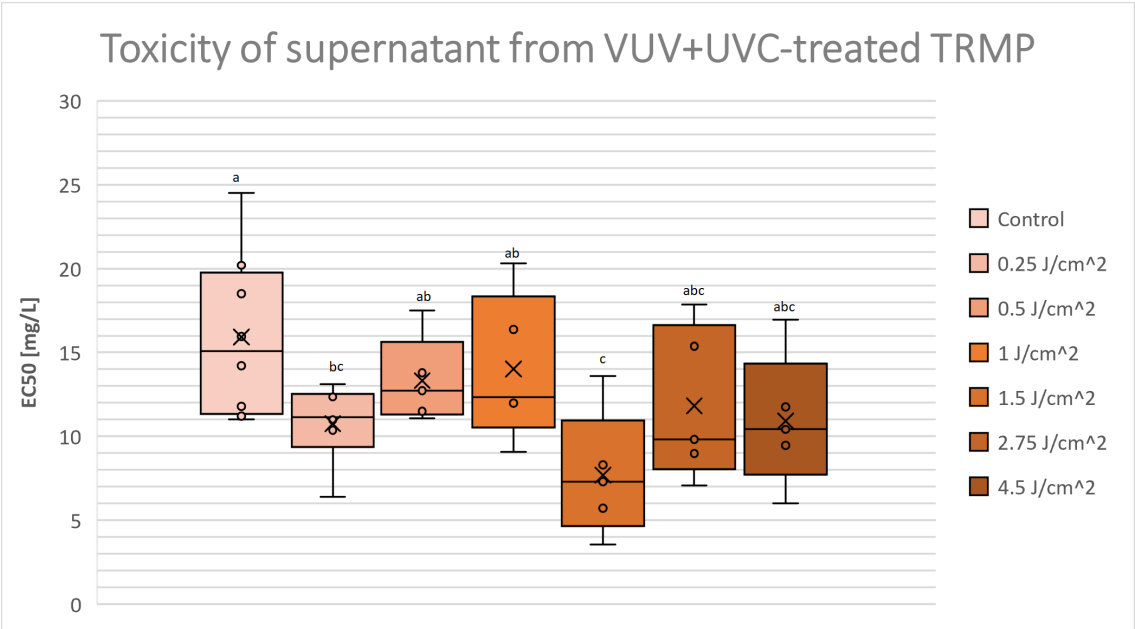

Figure 22. Boxplots showing EC50 from the control and different treatment intensities representing the toxicity of the supernatant from VUV+UVC treated TRMP. The boxplots have been assigned a letter depending on whether they are significantly different from each other with a P-value of <0.05.

The control has an average EC50 value of $15.92 \pm 4.54 \frac{mg}{L}$, while the samples treated with 0.25 $\frac{J}{cm^2}$ VUV+UVC, 0.5 $\frac{J}{cm^2}$VUV+UVC, 1 $\frac{J}{cm^2}$ VUV+UVC, $1.5\frac{J}{cm^2}$ VUV+UVC, $2.75\frac{J}{cm^2}$ VUV+UVC and $4.5\frac{J}{cm^2}$ VUV+UVC have average EC50 values of $10.75 \pm 2.14 \frac{mg}{L}$,

$13.32 \pm 2.29\frac{mg}{L}$, $14.04 \pm 2.99\frac{mg}{L}$, $7.69 \pm 3.36\frac{mg}{L}$, $11.83 \pm 4.09\frac{mg}{L}$, and $10.92 \pm 3.56\frac{mg}{L}$ respectively.

To see if there is any statistically significant difference between the non-UV treated supernatant, and the supernatant treated at different VUV+UVC intensities, a wilcoxon rank sum test was conducted. The results can be seen in table 4.

Table 4. P- values from wilcoxon rank sum test for the comparison of EC50 values between the different treatment intensities and no treatment with VUV+UVC. P<0.05 is marked with (*) and P<0.01 is marked with (**).

	Control	**0.25** $\frac{J}{cm^2}$	**0.5** $\frac{J}{cm^2}$	**1.0** $\frac{J}{cm^2}$	**1.5** $\frac{J}{cm^2}$	**2.75** $\frac{J}{cm^2}$	**4.5** $\frac{J}{cm^2}$
0.25 $\frac{J}{cm^2}$	0.039*	-					
0.5 $\frac{J}{cm^2}$	0.37	0.10	-				
1.0 $\frac{J}{cm^2}$	0.77	0.27	0.92	-			
1.5 $\frac{J}{cm^2}$	0.013*	0.20	0.047*	0.047*	-		
2.75 $\frac{J}{cm^2}$	0.11	1	0.46	0.35	0.12	-	
4.5 $\frac{J}{cm^2}$	0.079	0.72	0.17	0.25	0.17	0.92	-

From table 4 it can be seen that only two of the treatments are significantly different from the control, that being the treatment at $0.25\frac{J}{cm^2}$ and $1.5\frac{J}{cm^2}$ VUV+UVC. Table 4 also shows that the treatment at $1.5\frac{J}{cm^2}$ VUV+UVC are significantly different from treatment at $0.5\frac{J}{cm^2}$ and $1.0\frac{J}{cm^2}$ VUV+UVC.

Figure 23 shows the concentration of zinc released from TRMP treated with different doses of VUV+UVC and the non-treated control. The figure shows the concentration of Zn in $\frac{mg}{L}$, which is equivalent to mg zinc released per g of TRMP, since the solution of TRMP in tap water used is 1 $\frac{g}{L}$.

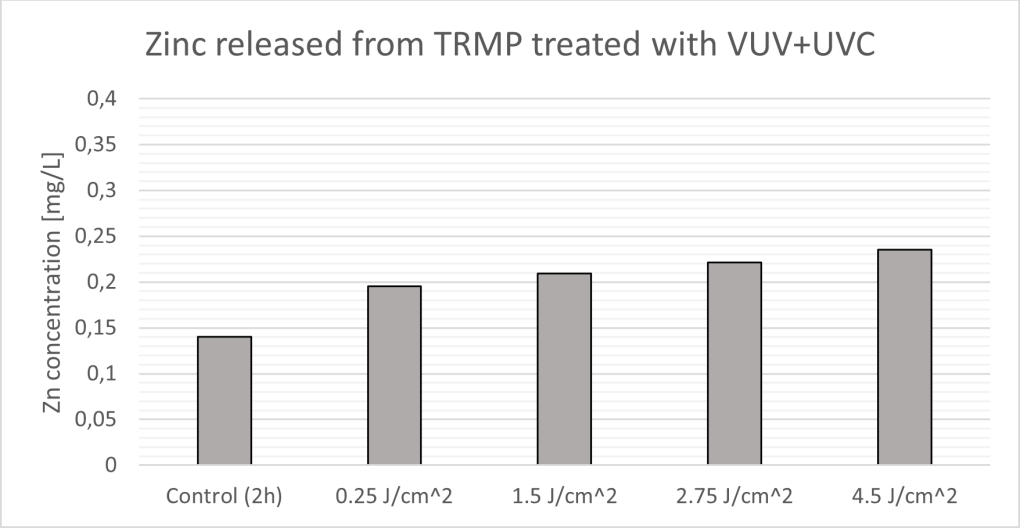

Figure 23. Zinc concentration in TRMP solutions treated with different doses of VUV+UVC. Determined with the photometric zinc test.

As seen from figure 23 the lowest measured zinc concentration was found in the control ($0.14\frac{mg}{L}$ Zn), while the highest concentration was measured in the TRMP treated with

$4.5\frac{J}{cm^2}$ VUV+UVC ($0.24\frac{mg}{L}$ Zn). Overall there is an increase in release of zinc from the TRMP when exposed to increasing doses of VUV+UVC.

Figure 24 shows the release of the three PAHs fluoranthene, pyrene and BaP from TRMP solutions treated with VUV+UVC at different doses.

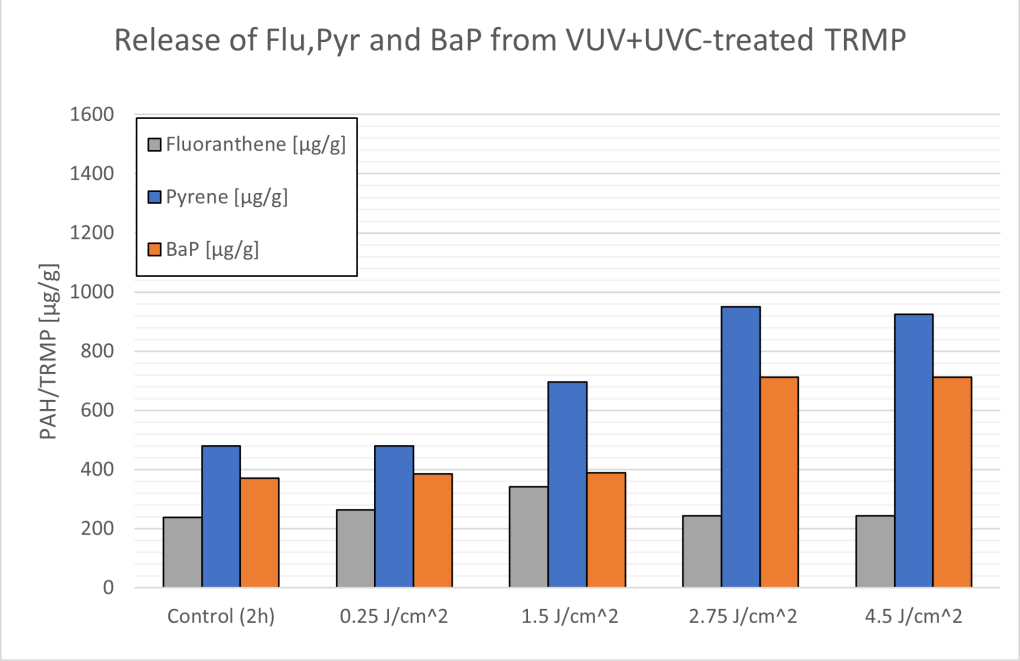

Figure 24. The release of fluoranthene, pyrene and BaP in TRMP solutions treated with different doses of VUV+UVC. Expressed in μg PAH per g of TRMP.

Figure 24 shows an increase in release of the PAHs pyrene and BaP from the TRMP when exposed to increasing doses of VUV+UVC, not observed for fluoranthene.

4.3 Comparison of UVC and VUV+UVC treatment

To see if there is any difference in toxicity between the treatments with UVC only and the treatments with VUV+UVC a comparison was made between the toxicity of supernatant treated with the same intensity. The results of this comparison can be seen in figure 25.

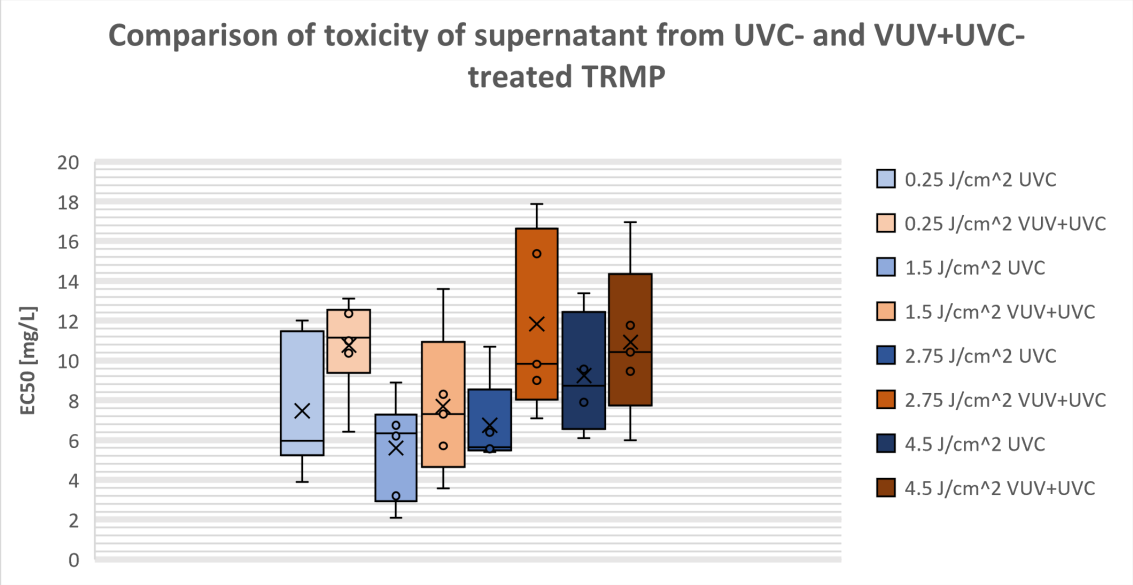

Figure 25. Boxplots comparing the EC50 for UVC and VUV+UVC treatments of TRMP supernatant effect on *R. subcapitata*.

In table 5 the p-value of the wilcoxon rank sum test for the comparison between UVC and VUV+UVC treatment can be seen. From the table it is only the treatment at $2.75\frac{J}{cm^2}$ where there is a significant difference between UVC and VUV+UVC treatment.

Table 5. P- values from wilcoxon rank sum test for the comparison of EC50 values between UVC and VUV+UVC with the same treatment intensities. P<0.05 is marked with (*) and P<0.01 is marked with (**).

	$\mathbf{0.25\frac{J}{cm^2}}$	$\mathbf{1.5\frac{J}{cm^2}}$	$\mathbf{2.75\frac{J}{cm^2}}$	$\mathbf{4.5\frac{J}{cm^2}}$
P-value	0.078	0.18	0.047*	0.62

4.4 Effect of UV treatment on 21d particle free TRMP leachate on metals, PAHs and toxicity

The supernatant from the 1L TRMP solution with an original concentration of 1 $\frac{g}{L}$ TRMP, were treated with similar intensities of UV as in the experiments with TRMP particles treated with UV. The supernatant was centrifuged and filtered, so no particles were present before being treated with UV. The following are the results of these experiments.

4.4.1 Treatment with UVC

Figure 26 shows all growth inhibition curves from different treatments with UVC. In the figure is the inhibition curve for the 21 day control and supernatant treated with 0.25 $\frac{J}{cm^2}$ UVC, $1.5\frac{J}{cm^2}$ UVC, $2.75\frac{J}{cm^2}$ UVC and $4.5\frac{J}{cm^2}$ UVC respectively. All data points are plotted alongside the inhibition curves.

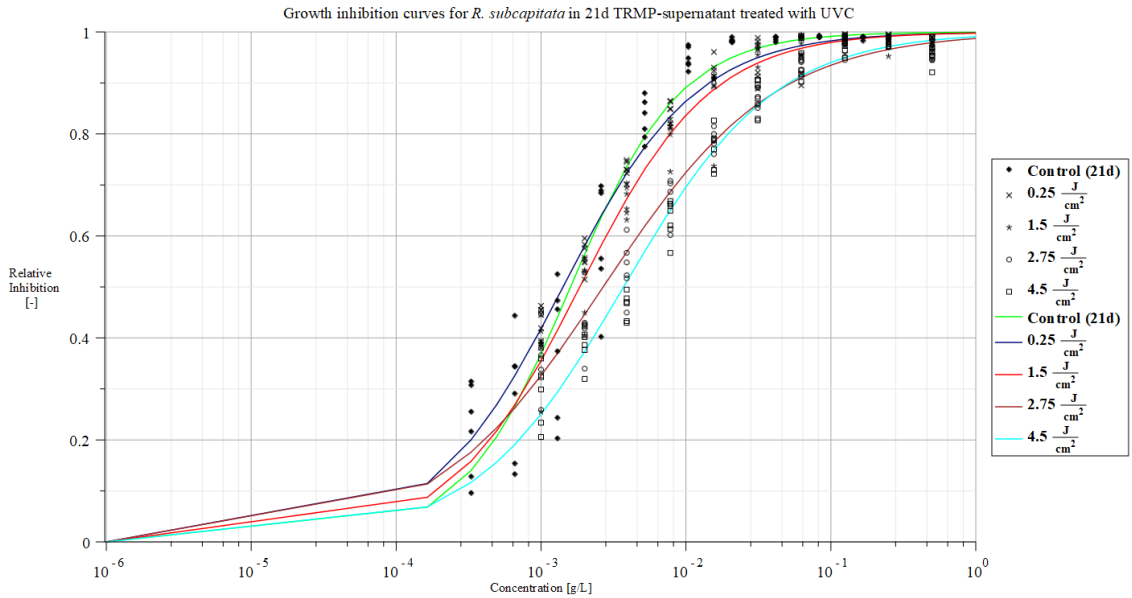

Figure 26. Growth inhibiton curves for *R. subcapitata* exposed to supernatant from a 21d TRMP solution treated with different doses of UVC.

There is a shift towards the right for the curves that indicate a decrease in toxicity with an increased dose of UVC. The curves are made from 3 replicates made independently from each other of the same intensity for each treatment. The control is also made from 3 replicates.

From the growth inhibition curves in figure 26 EC50 values were obtained for the different treatments. The results of this can be seen in figure 27.

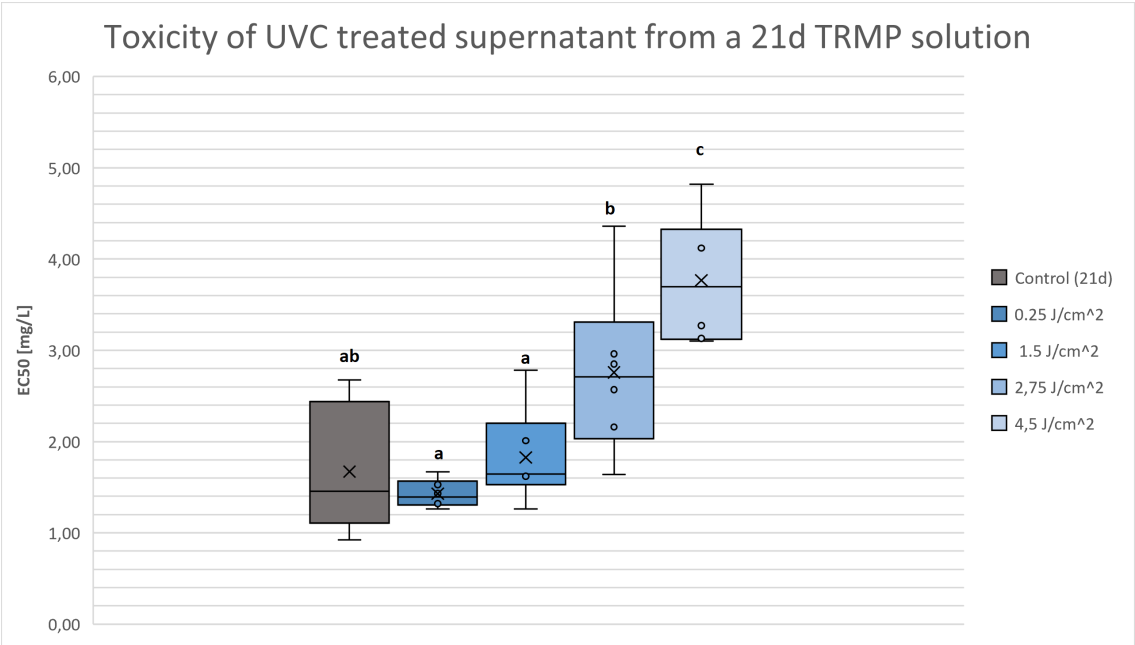

Figure 27. Boxplots showing EC50 from the control (21d) and TRMP-supernatant treated with different doses of UVC. The EC50 values are given in mg/L representing the dilution from the original TRMP solution with 1 g/L TRMP. The boxplots have been assigned a letter depending on whether they are significantly different from each other with a P-value of <0.05.

The control has an average EC50 value of $1.67 \pm 0.65 \frac{mg}{L}$, while the samples treated with 0.25 $\frac{J}{cm^2}$ UVC, $1.5 \frac{J}{cm^2}$ UVC, $2.75 \frac{J}{cm^2}$ UVC and $4.5 \frac{J}{cm^2}$ UVC have average EC50 values of $1.4 \pm 0.14 \frac{mg}{L}$, $1.83 \pm 0.48 \frac{mg}{L}$, $2.76 \pm 0.84 \frac{mg}{L}$, and $3.77 \pm 0.64 \frac{mg}{L}$ respectively. The concentration in mg/L relates to the dilution from the original TRMP solution with 1 g/L TRMP.

In order to figure out if there is any statistically significant difference between the non-UV treated supernatant, and the supernatant treated at different UVC intensities, a wilcoxon rank sum test was conducted. The results can be seen in table 6.

Table 6. P- values from wilcoxon rank sum test for the comparison of EC50 values between the different treatment intensities and no treatment with UVC. P<0.05 is marked with (*) and P<0.01 is marked with (**).

	Control	**0.25** $\frac{J}{cm^2}$	**1.5** $\frac{J}{cm^2}$	**2.75** $\frac{J}{cm^2}$
0.25 $\frac{J}{cm^2}$	1	-		
1.5 $\frac{J}{cm^2}$	0.52	0.13	-	
2.75 $\frac{J}{cm^2}$	0.055	0.0065**	0.037*	-
4.5 $\frac{J}{cm^2}$	0.0039**	0.0040**	0.0040**	0.037*

Table 6 shows that there is a significant difference between the EC50 values of the control and the supernatant treated with $4.5 \frac{J}{cm^2}$ UVC, while also showing significant difference between supernatant treated with different doses of UVC.

Figure 28 shows the concentration of zinc in the supernatant before treatment with UVC and after treatment with different doses of UVC . The figure shows the concentration of Zn in $\frac{mg}{L}$.

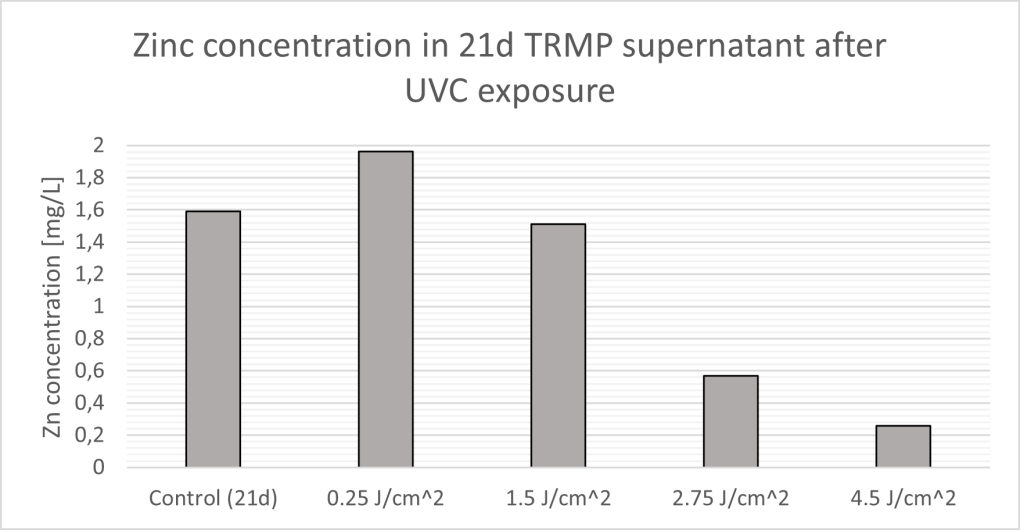

Figure 28. Zinc concentration in supernatant treated with different doses of UVC. Determined with the photometric zinc test.

As seen from figure 28 the lowest measured zinc concentration was found in the supernatant treated with $4.5 \frac{J}{cm^2}$ UVC ($0.26 \frac{mg}{L}$ Zn), while the highest concentration was measured in

the supernatant treated with 0.25 $\frac{J}{cm^2}$ UVC (1.96$\frac{mg}{L}$ Zn). Overall there is decrease in Zn concentration in the supernatant when exposed to increasing doses of UVC.

Figure 29 shows the removal of the three PAHs fluoranthene, pyrene and BaP from supernatant treated with UVC at different doses.

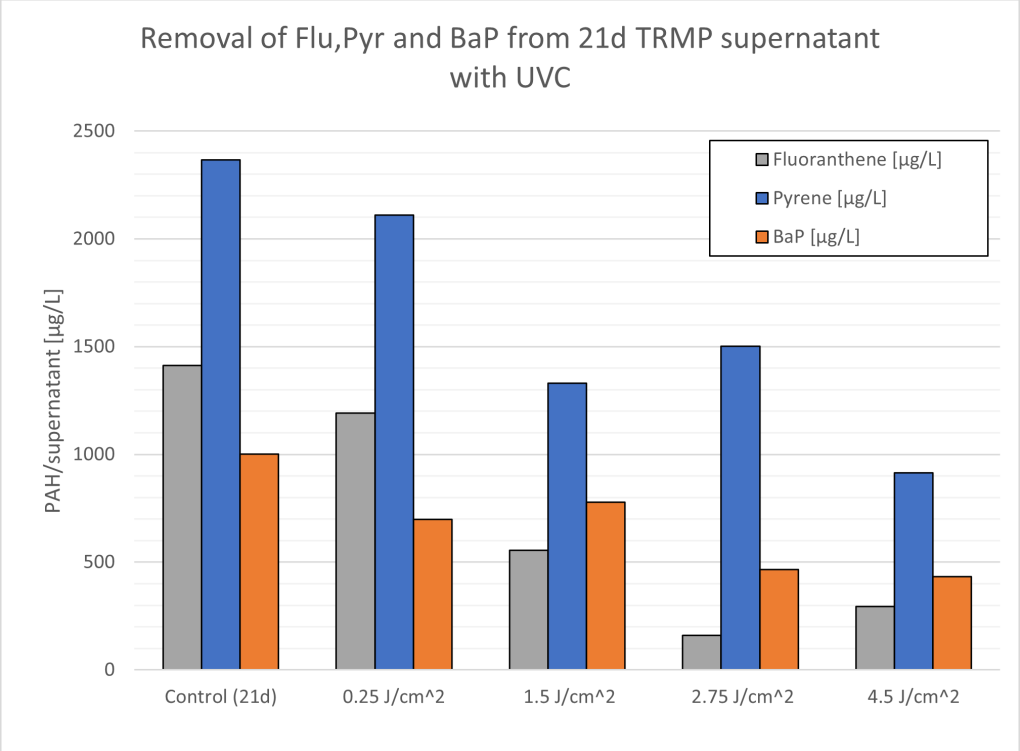

Figure 29. The removal of fluoranthene, pyrene and BaP in supernatant treated with different doses of UVC. Expressed in μg PAH per L.

Figure 29 shows a decrease in concentration of PAH in the supernatant when exposed to increasing doses of UVC.

4.4.2 Treatment with VUV+UVC

Figure 30 shows all growth inhibition curves from different treatments with VUV+UVC. In the figure is the inhibition curve for the 21 day control and supernatant treated with 0.25 $\frac{J}{cm^2}$ VUV+UVC, 1.5$\frac{J}{cm^2}$ VUV+UVC, 2.75$\frac{J}{cm^2}$ VUV+UVC and 4.5$\frac{J}{cm^2}$ VUV+UVC respectively. All data points are plotted alongside the inhibition curves.

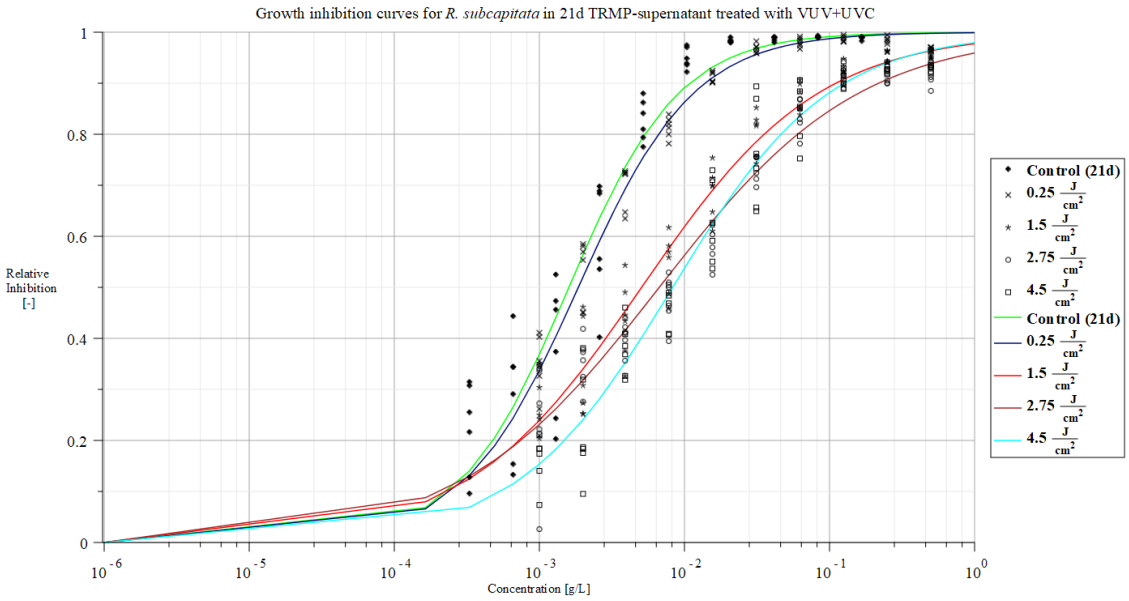

Figure 30. Growth inhibiton curves for *R. subcapitata* exposed to supernatant from a 21d TRMP solution treated with different doses of VUV+UVC

There is a shift towards the right for the curves that indicate a decrease in toxicity with an increased dose of VUV+UVC. The curves are made from 3 replicates made independently from each other of the same intensity for each treatment. The control is also made from 3 replicates.

From the growth inhibition curves in figure 30 EC50 values were obtained for the different treatments. The results of this can be seen in figure 31.

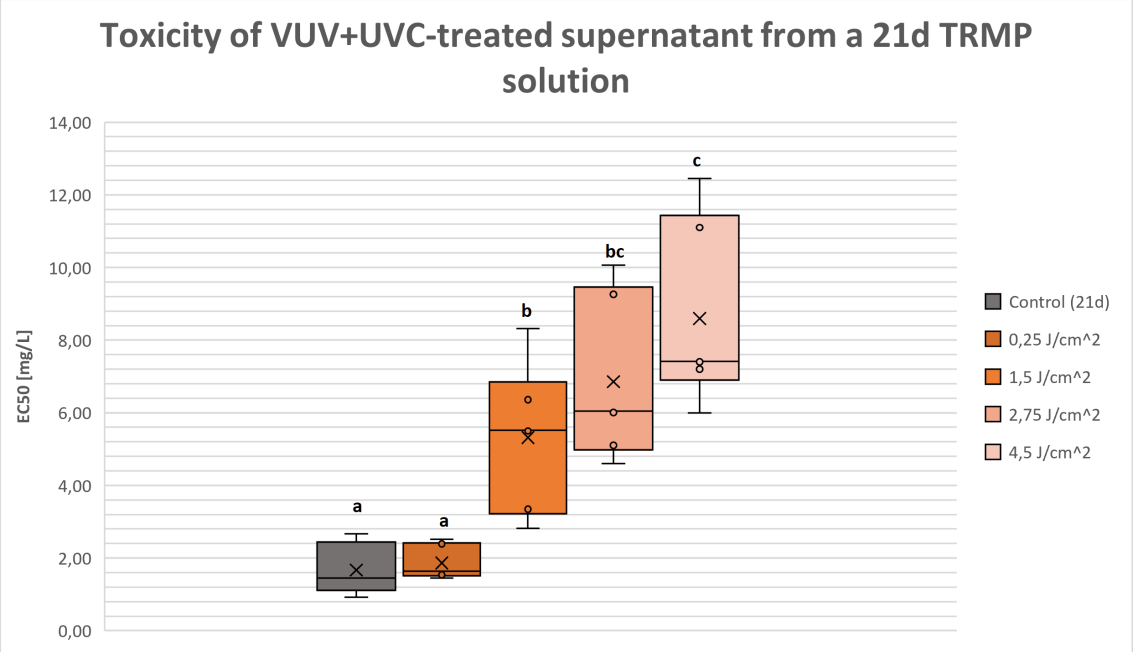

Figure 31. Boxplots showing EC50 from the control (21d) and TRMP-supernatant treated with different doses of VUV+UVC. The EC50 values are given in mg/L representing the dilution from the original TRMP solution with 1 g/L TRMP. The boxplots have been assigned a letter depending on whether they are significantly different from each other with a P-value of <0.05.

The control has an average EC50 value of $1.67 \pm 0.65 \frac{mg}{L}$, while the samples treated with 0.25 $\frac{J}{cm^2}$ VUV+UVC, $1.5 \frac{J}{cm^2}$ VUV+UVC, $2.75 \frac{J}{cm^2}$ VUV+UVC and $4.5 \frac{J}{cm^2}$ VUV+UVC have average EC50 values of $1.86 \pm 0.43 \frac{mg}{L}$, $5.32 \pm 1.84 \frac{mg}{L}$, $6.85 \pm 2.06 \frac{mg}{L}$, and $8.60 \pm 2.33 \frac{mg}{L}$ respectively. The concentration in mg/L relates to the dilution from the original TRMP solution with 1 g/L TRMP.

In order to figure out if there is any statistically significant difference between the non-UV treated supernatant and the supernatant treated at different UVC intensities a wilcoxon rank sum test was conducted. The results can be seen in table 7.

Table 7. P- values from wilcoxon rank sum test for the comparison of EC50 values between the different treatment intensities and no treatment with VUV+UVC. $P<0.05$ is marked with (*) and $P<0.01$ is marked with (**).

	Control	**0.25** $\frac{J}{cm^2}$	**1.5** $\frac{J}{cm^2}$	**2.75** $\frac{J}{cm^2}$
0.25 $\frac{J}{cm^2}$	0.52	-		
1.5 $\frac{J}{cm^2}$	0.0039**	0.0039**	-	
2.75 $\frac{J}{cm^2}$	0.0039**	0.0039**	0.34	-
4.5 $\frac{J}{cm^2}$	0.0039**	0.0039**	0.038*	0.2

Table 7 shows that there is a significant difference between the EC50 values of the control and the supernatant treated with $1.5 \frac{J}{cm^2}$ VUV+UVC, $2.75 \frac{J}{cm^2}$ VUV+UVC and $4.5 \frac{J}{cm^2}$ VUV+UVC, while also showing significant difference between supernatant treated with different doses of VUV+UVC.

Figure 32 shows the concentration of zinc in the supernatant before treatment with

VUV+UVC and after treatment with different doses of VUV+UVC . The figure shows the concentration of Zn in $\frac{mg}{L}$.

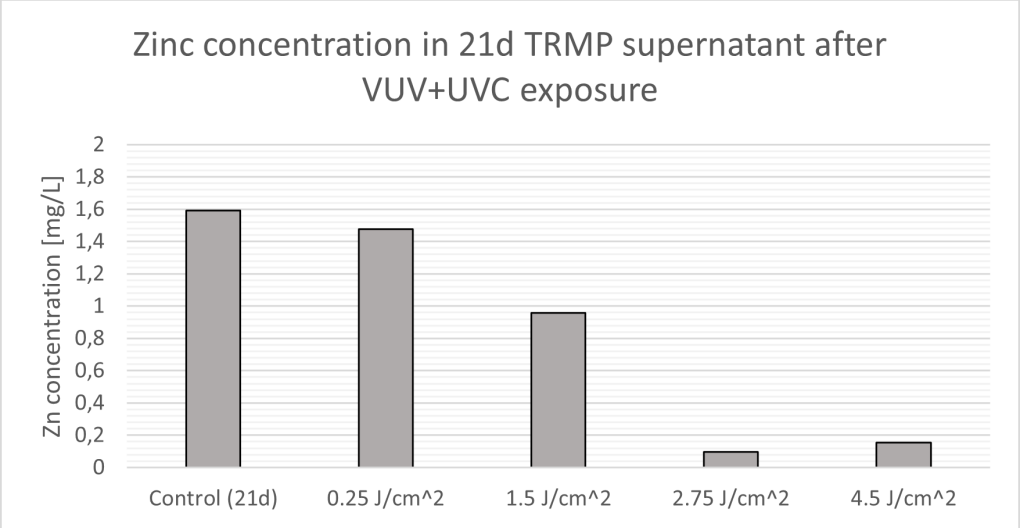

Figure 32. Zinc concentration in supernatant treated with different doses of VUV+UVC. Determined with the photometric zinc test.

As seen from figure 32 the lowest measured zinc concentration was found in the supernatant treated with $2.75\frac{J}{cm^2}$ VUV+UVC ($0.098\frac{mg}{L}$ Zn), while the highest concentration was measured in the supernatant without treatment ($1.59\frac{mg}{L}$ Zn). Overall there is decrease in Zn concentration in the supernatant when exposed to increasing doses of VUV+UVC.

Figure 33 shows the removal of the three PAHs fluoranthene, pyrene and BaP from supernatant treated with VUV+UVC at different doses.

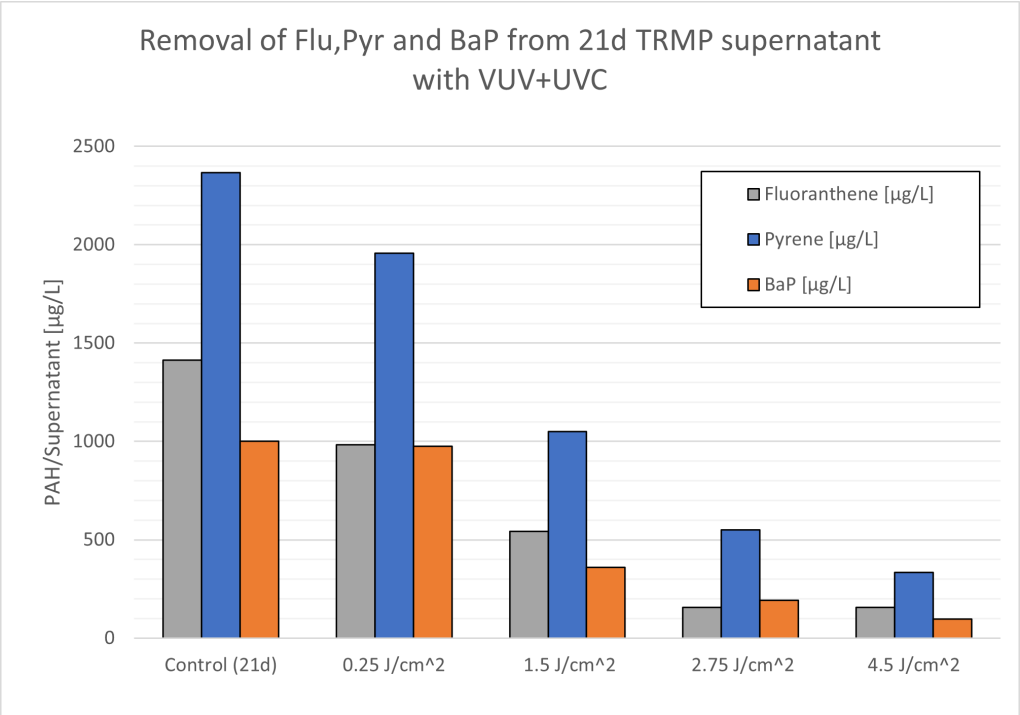

Figure 33. The removal of fluoranthene, pyrene and BaP in supernatant treated with different doses of VUV+UVC. Expressed in μg PAH per L.

Figure 33 shows a decrease in concentration of PAH in the supernatant when exposed to increasing doses of VUV+UVC.

4.4.3 Comparison of toxicity between UVC and VUV+UVC treatment

To see if there is any difference in toxicity between the treatments with UVC only and the treatments with VUV+UVC a comparison was made between the toxicity of supernatant treated with the same doses of UVC and VUV+UVC. The results of this comparison can be seen in figure 34.

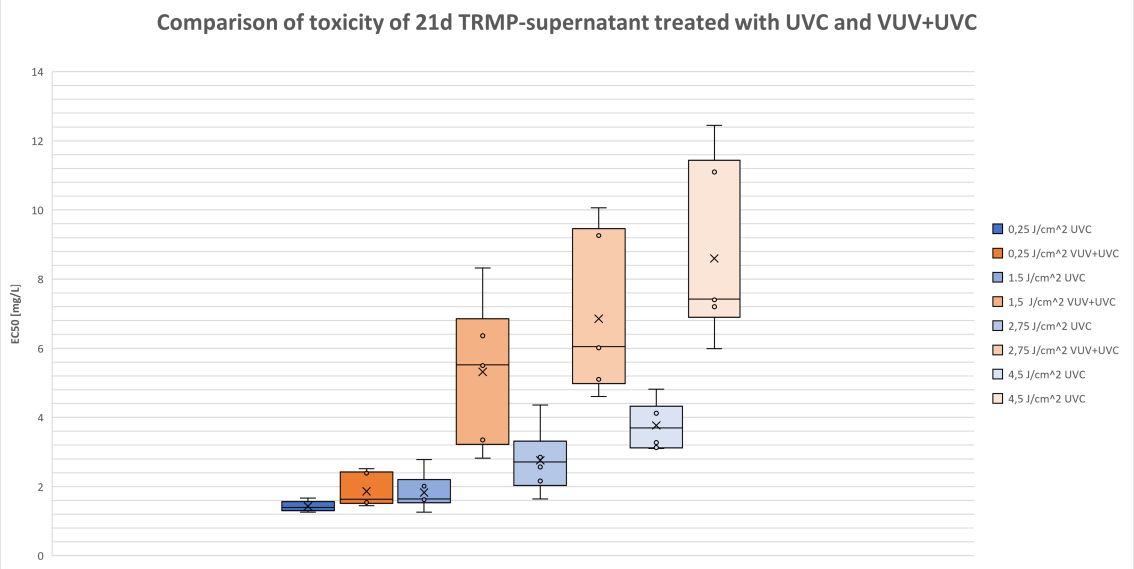

Figure 34. Boxplots comparing the EC50 for UVC and VUV+UVC treatments on the supernatant from the 21 day TRMP solution.

In table 8 the p-value of the wilcoxon rank sum test for the comparison between UVC and VUV+UVC treatment can be seen. From the table it is seen that there is a significant difference between treatment with UVC and treatment with VUV+UVC for all doses of UV.

Table 8. P- values from wilcoxon rank sum test for the comparison of EC50 values between UVC and VUV+UVC with the same treatment intensities. P<0.05 is marked with (*) and P<0.01 is marked with (**).

	$\mathbf{0.25}\frac{J}{cm^2}$	$\mathbf{1.5}\frac{J}{cm^2}$	$\mathbf{2.75}\frac{J}{cm^2}$	$\mathbf{4.5}\frac{J}{cm^2}$
P-value	0.0374*	0.0039**	0.0039**	0.0039**

5 Discussion

Toxicity of the leachates from TRMP particles treated with UVC expressed as EC50 values of the growth inhibition of *R. subcapitata* are shown in figure 18. The figure shows along with table 3 that the TRMP particles have released more toxic compounds under 254 nm UVC radiation compared to the non-irradited particles. This is in accordance with other studies where UV light is used to artificially age MP causing them to release more of their additives into the water [Sørensen et al., 2021]. This is well documented for natural occurring wavelengths of UV on MP, but not that many studies have used UVC wavelengths as weathering on TRMP. One study by Simon et al. [2021] have looked at different MP particles (including TRMP) and used UVC as a way to simulate accelerated weathering on particles in the same size range as this study (70 - 150 nm). Simon et al. [2021] even used the same test organism, *R. subcapitata*, as a toxicity indicator. Simon et al. [2021] similarly found that UVC irradiation increased the toxicity of TRMP leachates on *R. subcapitata*. The present study finds higher toxicity for the non-treated TRMP after 2 hours of leaching (EC50 = $15.92 \pm 4.54 \frac{mg}{L}$) than found in Simon et al. [2021] (EC50 = $470 \pm 40 \frac{mg}{L}$), even though they use a longer leaching time (72h). This could be explained by the smaller size fraction of TRMP used in this study, causing a larger surface area to size ratio for toxicants to leach through. Although UVC radiation induced higher toxicity for *R. subcapitata*, there did not seem to be any difference in toxicity for high or low doses of UVC.

The toxicity of leachates from treatment of TRMP with VUV/UVC expressed as EC50 values for growth inhibition of *R. subcapitata* are shown in figure 22. There is not the same significant change in toxicity for particles treated with VUV/UVC as there is for particles treated with UVC only. The table 4 also shows that there only is a significant difference between the non-irradiated control and the particles treated with $0.25 \frac{J}{cm^2}$ and $1.5 \frac{J}{cm^2}$ VUV/UVC. The radiation from the 185 nm VUV only constitutes 10% of the total UV radiation the remaining 90% comes from the 254 nm UVC. Looking at figure 25 all mean values of EC50 for the leachates from particles treated with VUV/UVC are higher than for those treated with UVC only when comparing particles treated with the same dose of UV. This is either an indication of UVC being more effective at breaking down TRMP and releasing leachates from the particles than VUV, or it indicates that VUV is more effective at removing compounds in leachates than UVC. From what was found by Yang et al. [2018] in relation to pesticide removal from water with UVC and VUV/UVC, and findings yet to be discussed in the present study, the latter seems to be more likely.

It was found that 140 $\frac{\mu g}{g}$ of zinc leached from the TRMP particles after 2 hours of leaching without UV irradiation. From figure 19 it is possible to estimate a linear rate of the leaching of zinc from TRMP when irradiated with UVC based on the additional amount of zinc

leached after irradiation. The rate of Zn release from TRMP is 46 $\frac{\mu g/g}{J/cm^2}$ UVC. A similar rate can be calculated for zinc leaching from TRMP irradiated with VUV/UVC using the values from figure 23. Zinc leaches at a rate of 16 $\frac{\mu g/g}{J/cm^2}$ VUV/UVC. The higher leaching rate of UVC irradiated TRMP compared to VUV/UVC irradiated TRMP is reflected in the higher toxicity to *R. subcapitata* as seen in figure 25. Other studies on leaching of zinc from tire rubber has named it as the main contributor to toxicity in TRMP leachates [Rhodes et al., 2012; Lu et al., 2021; Simon et al., 2021; Wik et al., 2009]. Simon et al. [2021] found that 80 $\frac{\mu g}{L}$ (66-95) of Zn ions was the EC50 for growth inhibition of *R. subcapitata*. Muyssen and Janssen [2001] found the EC50 for zinc on growth inhibition on *R. subcapitata* to be $39 \pm 12 \frac{\mu g}{L}$. In the present study average EC50 of zinc was $2.54 \pm 1.63 \frac{\mu g}{L}$, concentrations much lower than previously reported. This indicates that it is likely not only zinc contributing to the toxicity of leachates from UVC and VUV/UVC treated TRMP particles. It is possible that there is some synergistic effect between reactive oxygen species created by UVC and VUV/UVC irradiation and the zinc leachates causing the zinc to be more toxic. It is also likely that there are unknown compounds created having synergistic toxicity effects on *R. subcapitata*.

The release of the PAHs fluoranthene, pyrene and BaP from TRMP irradiated with UVC are shown in figure 20. After 2 hours of leaching with no irradiation 238 $\frac{\mu g}{g}$, 480 $\frac{\mu g}{g}$ and 370 $\frac{\mu g}{g}$ leached from the TRMP of fluoranthene, pyrene and BaP respectively. Pyrene and fluoranthene are leaching in roughly the same proportions as they are found in tire rubber, with pyrene being roughly twice as abundant as fluoranthene [Diekman et al., 2019]. BaP leaching is relatively high compared to the amount leached of fluoranthene and pyrene. All three PAHs leach more from the TRMP after the particles are exposed to UVC, all three peaking at the $1.5 \frac{J}{cm^2}$ dose of UVC with concentrations of 1507 $\frac{\mu g}{g}$, 1470 $\frac{\mu g}{g}$ and 668 $\frac{\mu g}{g}$ leached from the TRMP of fluoranthene, pyrene and BaP respectively. This is also the dose where the EC50 is the lowest for UVC treated particles indicating a correlation between PAH concentration and toxicity to *R. subcapitata*. At the higher doses of UVC the concentration of leachates is lower than that at $1.5 \frac{J}{cm^2}$, although the final concentration at $4.5 \frac{J}{cm^2}$ is still higher than the control for all three PAHs. PAHs leaching from TRMP particles treated with VUV/UVC (figure 24) show the same tendency for more compounds leaching once treated with VUV/UVC. The concentrations are overall lower than that of leachates from UVC treated TRMP with the highest concentrations measured being 341 $\frac{\mu g}{g}$, 950 $\frac{\mu g}{g}$ and 711 $\frac{\mu g}{g}$ from fluoranthene, pyrene and BaP respectively. When analysing the data from the gas chromatography it became clear that there were multiple spikes representing different PAHs not included in the test, with some showing higher peaks than the PAHs included. It is believed that the three PAHs included in this study is representative for the overall concentration of PAHs leaching from the TRMP.

The experiments with the supernatant from the TRMP solution that had been leaching for 21 days, was a way to measure the removal of toxic compounds by UVC and VUV/UVC. After 21 days of leaching the EC50 was at $1.67 \pm 0.65 \frac{mg}{L}$ compared to the EC50 after 2 hours of leaching $15.92 \pm 4.54 \frac{mg}{L}$, making the 21 day leachate 10 times more toxic than the 2 hour control used in the experiments with UV induced leaching. The removal of toxicity with UVC can be seen in figure 27. The figure shows that UVC has a positive effect on the

removal of toxic compounds from the increasing values of EC50 with increased irradiation dose of UVC, with the EC50 being the highest at $3.77 \pm 0.64 \frac{mg}{L}$ for the highest dose of UVC at $4.5 \frac{J}{cm^2}$. The figure along with table 6 shows that there not only is a significance difference between the non-treated leachate and the leachate treated with $4.5 \frac{J}{cm^2}$ UVC, but also between the leachate treated with $4.5 \frac{J}{cm^2}$ UVC and the other doses of UVC. This indicates that the removal of toxicants is still happening even after long exposure to UVC. This is further supported by the fact that the leachate treated with $4.5 \frac{J}{cm^2}$ UVC is still more toxic than any of the supernatants from the experiments with UVC and VUV/UVC induced leaching.

The same control was used for removal of toxic compounds in the leachate with UVC and VUV/UVC, the removal toxic compounds however is very different. From figure 31 it can be seen that the VUV/UVC also has a positive effect on the removal of toxic compounds from the TRMP supernatant. With a significant difference between treated supernatant and the control at a dose of $1.5 \frac{J}{cm^2}$ VUV/UVC. This is different from the treatment with UVC were there only was a significant difference between the control and treatment with $4.5 \frac{J}{cm^2}$ UVC. Similarly as for the UVC treatment there is also a significant difference in EC50 between the different doses of VUV/UVC treatment indicating that removal of toxicants is still taking place even at the higher doses of VUV/UVC. The highest EC50 is found in the supernatant treated with $4.5 \frac{J}{cm^2}$ at $8.60 \pm 2.33 \frac{mg}{L}$. This EC50 is within the range of some of the values measured during the UVC and VUV/UVC induced leaching experiments. Looking at the figure 34 there is a clear significant difference between all treatments with UVC and VUV/UVC, when comparing similar doses, as it can be also seen in table 8. VUV/UVC is much more efficient at removing toxicants from the supernatant than only UVC, despite the VUV wavelength only delivering 10% of the UV dose. This also further supports the explanation that fewer toxic compounds are leaching from the VUV/UVC treated particles than from the UVC treated particles, because VUV/UVC is more efficient at removing them.

The removal of fluoranthene, pyrene and BaP from the particle free leachate with UVC are shown in figure 29. After 21 days of leaching the concentrations in the control are 1413 $\frac{\mu g}{L}$ for fluoranthene, 2366 $\frac{\mu g}{L}$ for pyrene and 1000 $\frac{\mu g}{L}$ for BaP. These concentrations are 5.9, 4.9 and 2.7 times higher respectively than the concentrations measured in the 2 hour leaching control in the experiments with UVC and VUV/UVC induced leaching. After the highest dose UVC the concentrations are 295 $\frac{\mu g}{L}$ for fluoranthene, 915 $\frac{\mu g}{L}$ for pyrene and 432 $\frac{\mu g}{L}$ for BaP. That equals to a 79% removal for fluoranthene, a 61% removal for pyrene and a 56% removal for BaP. This follows the findings by Rosinska [2021] in removing PAH's from wastewater. Rosinska [2021] used much lower concentrations in the ng/L range and therefore it might be the reason why they find a cap in removal around 30 minutes of exposure to UVC, while in this study the removal seems to happen continuously. The removal of PAHs with VUV/UVC as shown in figure 33 shows that all three PAHs are being removed under exposure with VUV/UVC. After the highest dose of $4.5 \frac{J}{cm^2}$ VUV/UVC the concentrations are 155 $\frac{\mu g}{L}$ for fluoranthene, 335 $\frac{\mu g}{L}$ for pyrene and 96 $\frac{\mu g}{L}$ for BaP, which is lower than the leaching from the 2 hour control. That equals to a 89% removal for fluoranthene, a 86% removal for pyrene and a 90% removal for BaP after

$4.5\frac{J}{cm^2}$ VUV/UVC. This removal is more efficient than the one observed with only UVC. If the three PAHs are a measure for the total amount of PAHs removed then VUV/UVC is 2% better than UVC at $0.25\frac{J}{cm^2}$, 27% better at $1.5\frac{J}{cm^2}$, 58% better at $2.75\frac{J}{cm^2}$ and 64% better at $4.5\frac{J}{cm^2}$. The comparison of removal of PAHs between UVC and VUV/UVC follows the overall trends seen in the comparison of toxicity in figure 34, indicating that PAHs are a factor in the toxicity of TRMP leachates.

The figures 28 and 32 show the concentration of zinc in the UVC and VUV/UVC treated supernatant. After 21 days of leaching the concentration of zinc is 1591 $\frac{\mu g}{L}$, which is 11.3 times more than the concentration measured in the 2 hour leaching control in the experiments with UVC and VUV/UVC induced leaching. Both UVC and VUV/UVC irradiation causes the concentration of zinc to be lowered down to a concentration of 258 $\frac{\mu g}{L}$ for UVC and 154 $\frac{\mu g}{L}$ for VUV/UVC at a irradiation dose of $4.5\frac{J}{cm^2}$. The explanation for this apparent removal of zinc is hard to find in the literature and it should not be possible for the zinc ions to disappear or evaporate from the supernatant. A plausible explanation is that UVC and VUV/UVC causes zinc to form organic compounds that precipitate in the water, fx. ZnO, ZnO_2 or $Zn(OH)_2$. This explanation is plausible if not all of the sample is extracted after ended exposure. For both UVC and VUV/UVC all of the sample was extracted when used in the zinc test. Therefore this result mandates further research into the fate of zinc compounds under the irradiation of UVC and VUV/UVC.

The doses of UVC and VUV/UVC used in this report are relatively high compared to what is typically used for disinfection of a WWTP. According to Hinjen et al. [2006] the dose used for proper disinfection in WWTPs is 100 - 200 $\frac{mJ}{cm^2}$. The lowest exposure used in the experiments of this study are 250 $\frac{mJ}{cm^2}$, which is somewhat comparable to the actual doses, while the highest dose of 4500 $\frac{mJ}{cm^2}$ is 22.5-45 times higher than what is used in WWTPs. In this study no significant effect was found for samples treated with 250 $\frac{mJ}{cm^2}$ UVC and VUV/UVC, but significant effects were found both for leaching and removal of leachates from TRMP at 4500 $\frac{mJ}{cm^2}$ UVC and VUV/UVC. This is similar to what Lin et al. [2020] found when looking at surface degradation of microplastics, with the recommended dose having little effect while a dose 20 times higher had significant effects on the surface degradation.

Other studies investigating leaching of toxic compounds from TRMP have used larger pieces of rubber mulch and have therefore found lower leaching products than in this report. The size of $<125\ \mu m$ particles in this report are comparable to the particles found in the environment from car tire abrasion.

6 Conclusion

This study investigated the effects that UVC and VUV/UVC irradiation have on the leaching of toxic compounds from TRMP particles and the effects that UVC and VUV/UVC irradiation have on the removal of these compounds from the water.

It was found that both UVC and VUV/UVC irradiation causes toxic compounds to leach from TRMP particles with a EC50 for the microalgae *R. subcapitata* in the range of 5.61 - 9.24 $\frac{mg}{L}$ for UVC irradiated TRMP particles and 7.69 - 14.04 $\frac{mg}{L}$ for VUV/UVC irradiated TRMP particles. In comparison, non-UV treated particles showed EC50 of $15.92 \pm 4.54 \frac{mg}{L}$.

UVC and VUV/UVC irradiation caused zinc and PAHs to leach from the TRMP particles. Zinc leached at a rate of 46 $\frac{\mu g/g}{J/cm^2}$ for UVC irradiation and at a rate of 16 $\frac{\mu g/g}{J/cm^2}$ for VUV/UVC irradiation. The three PAHs investigated (fluoranthene, pyrene and benzo(a)pyrene) all leached more from the TRMP particles under UVC irradiation than for those under VUV/UVC irradiation.

VUV/UVC proved to be more efficient in the removal of toxic compounds from TRMP leachate than UVC. With the non-irradiated leachate having a EC50 for *R. subcapitata* at $1.67 \pm 0.65 \frac{mg}{L}$. The EC50 for the leachates after the highest dose of UV irradiation was $3.77 \pm 0.64 \frac{mg}{L}$ for UVC and $8.60 \pm 2.33 \frac{mg}{L}$ for VUV/UVC. VUV/UVC removed 89% of fluoranthene, 86% of pyrene and 90% of benzo(a)pyrene from the leachate at the highest dose, while UVC only removed 79% of fluoranthene, 61% of pyrene and 56% of benzo(a)pyrene at the highest dose.

With more and more tire waste rubber ending up in the aquatic environment through the waste water processing, it is important to understand the effects that UVC and VUV/UVC disinfection can have on these particles and their leachates. VUV have been shown to remove many different environmental pollutants in waste- and drinking water. This study shows that VUV/UV is also effective at removing toxic compounds from TRMP leachates, which can contribute to reduce the toxic load these particles have on the environment if this technology are implemented in water treatment.

More research is needed to understand the effect of UVC and VUV/UVC irradiation on the fate of dissolved zinc compounds and their bioavailability.

Bibliography

ATSDR, 2005. *Toxicological profile for Zinc.* `https://wwwn.cdc.gov/TSP/ToxProfiles/ToxProfiles.aspx?id=302&tid=54`. Downloaded: 05-05-2022.

Baensch-Baltruschat, B., Kocher, B., Stock, F. and Reifferscheid, G., 2020. *Tyre and road wear particles (TRWP) - A review of generation, properties, emissions, human health risk, ecotoxicity, and fate in the environment.* Science of the Total Environment, 733, 137823. doi: 10.1016/j.scitotenv.2020.137823.

Banerjee, S., Mandal, A. and Rooby, J., 2016. *Studies on Mechanical Properties of Tyre Rubber Concrete.* SSRG International Journal of Civil Engineering, 3, 6–9. doi: 10.14445/23488352/IJCE-V3I7P103.

Broeke, H.T., Hulskotte, J. and van der Gon, H.A.C. Denier, 2008. *Netherlands National Water Board – Water Unit, (Eds.) Road Traffic Tire Wear. Emission Estimates for Diffuse Sources.* Netherlands Emission Inventory. TNO Built Environment and Geosciences.

Burleigh, T.D., Ruhe, C. and Forsynth, J., 2003. *Photo-Corrosion of Different Metals during Long-Term Exposure to Ultraviolet Light.* Corrosion, 59, 774–779. doi: 10.5006/1.3277606.

Capolupo, M., Sørensen, L., Jayasena, K.D.R., Booth, A.M. and Fabbri, E., 2020. *Chemical composition and ecotoxicity of plastic and car tire rubber leachates to aquatic organisms.* Water Research, 169, 115270. doi: 10.1016/j.watres.2019.115270.

Cataldo, F., Ursini, O. and Angelini, G., 2010. *Surface oxidation of rubber crumb with ozone.* Polymer Degradation and Stability, 95, 803–810. doi: 10.1016/j.polymdegradstab.2010.02.003.

Chen, B., Huang, Y., Zhang, Q., Dionysio, D.D., Wang, L. and Li, J., 2021. *Formation of Nitrite and Hydrogen Peroxide in Water during the Vacuum Ultraviolet Irradiation Process: Impacts of pH, Dissolved Oxygen, and Nitrate Concentration.* Environmental Science and Technology, 55, 1682–1689. doi: 10.1021/acs.est.0c06161.

Claus, H., 2021. *Ozone Generation by Ultraviolet Lamps.* Photochemistry and photobiology, 97, 471–476. doi: 10.1111/php.13391.

Continental, 2014. *Tyre Basics Passenger Car Tyres*. Continental, https://blobs.continental-tires.com/www8/servlet/blob/585558/d2e4d4663a7c79ca81011ab47715e911/download-tire-basics-data.pdf.

Councell, T.B., Duckenfield, K.U., Landa, E.R. and Callender, E., 2004. *Tire-Wear Particles as a Source of Zinc to the Environment*. Environmental Science Technology, 38, 4206–4214. doi: 10.1021/es034631f.

Dannis, M.L., 1974. *Rubber Dust from the normal Wear of Tires*. Environmental Science Technology, 47, 1011–1037. doi: doi.org/10.5254/1.3540458.

Diekman, A., Giese, U. and Schauman, I., 2019. *Polycyclic aromatic hydrocarbons in consumer goods made from recycled rubber materia: A review*. Chemosphere, 202, 1163–1178. doi: 10.1016/j.chemosphere.2018.12.111.

Dillon, E., 2017. *The Effect of Temperature on Zinc Leaching from Rubber Tire Mulch*. Journal of the South Carolina Academy of Science, 15, 82–86.

Du, J., Wang, C., Zhao, Z., Cui, F., Ou, Q. and Lie, J., 2021. *Role of oxygen and superoxide radicals in promoting H2O2 production during VUV/UV radiation of water*. Chemical Engineering Science, 241, 116683. doi: 10.1016/j.ces.2021.116683.

Dumne, S.M., 2013. *An Experimental Study on Performance of Recycled Tyre Rubber-Filled Concrete*. International Journal of Engineering Research and Technology, 2, 766–772.

ETRMA, 2021a. *In Europe 95% of all End of Life Tyres were collected and treated in 2019 - Press Release*. European Tyre and Rubber Manufacturers Association, https://www.etrma.org/wp-content/uploads/2021/05/20210520_ETRMA_PRESS-RELEASE_ELT-2019.pdf.

ETRMA, 2021b. *European Tyre and Rubber Industry Statistics Edition 2021*. European Tyre and Rubber Manufacturers Association, https://www.etrma.org/wp-content/uploads/2021/12/20211215-Statistics-booklet-2021VF.pdf.

Evangeliou, N., Grythe, H., Klimont, Z., Heyes, C., Eckhardt, S., Lopez-Aparicio, S. and Stohl, A., 2020. *Atmospheric transport is a major pathway of microplastics to remote regions*. Nature Communications, 11, 3381. doi: 10.1038/s41467-020-17201-9.

GENAN, 2022. *GENAN 120 mesh sigteanalyse*. https://www.genan.eu/wp-content/uploads/2017/06/GENAN-120-Mesh_0-125-micron_DK.pdf. Downloaded: 03-05-2022.

Gewert, B., Plassmann, M. and MacLeod, M., 2015. *Pathways for degradation of plastic polymers floating in the marine environment*. Environmental Science Processes & Impacts, 17, 1513–1521. doi: 10.1039/c5em00207a.

Grigoratos, T. and Martini, G., 2014. *Non-Exhaust Traffic Related Emissions. Brake and Tyre Wear PM*. European Commission, Joint Research Centre, 26648 EN. doi: 10.2790/21481.

Halle, L.L., Palmqvist, A., Kampmann, K. and Khan, F.R., 2020. *Ecotoxicology of micronized tire rubber: Past, present and future considerations.* Science of the Total Environment, 706, 1–11. doi: 10.1016/j.scitotenv.2019.135694.

Hamdi, A., Abdelaziz, G. and Farhan, K.Z., 2021. *Scope of reusing waste shredded tires in concrete and cementitious composite materials: A review.* Journal of Building Engineering, 35, 1–30. doi: 10.1016/j.jobe.2020.102014.

Hartwell, S.I., Jordahl, D.M. and Dawson, C.E.O, 2000. *The Effect of Salinity on Tire Leachate Toxicity.* Water Air and Soil Pollution, 121, 119–131. doi: 10.1023/A:1005282201554.

Hinjen, W.A.M., Beerendonk, E.F. and Medema, G.J., 2006. *Inactivation credit of UV radiation for viruses, bacteria and protozoan (oo)cysts in water: A review.* Water Research, 40, 3–22. doi: 10.1016/j.watres.2005.10.030.

Holst, O., Stenberg, B. and Christiansson, M., 1998. *Biotechnological possibilities for waste tyre-rubber treatment.* Biodegradation, 9, 301–310.

ISO, 2013. *ISO 472:2013 Plastics - Vocabulary.* International Organization for Standardization.

ISO, 2012. *ISO 8692:2012 Water quality — Fresh water algal growth inhibition test with unicellular green algae.* International Organization for Standardization.

Jager, T.L.d, Cockrell, A.E. and Plessis, S.S.D. Ultraviolet Light Induced Generation of Reactive Oxygen Species. In *Ultraviolet Light in Human Health, Diseases and Environment.* Springer, 2017. doi: 10.1007/978-3-319-56017-5_2.

Kanematsu, M., Hayashi, A., Denison, M.S. and Young, T.M., 2009. *Characterization and potential environmental risks of leachate from shredded rubber mulches.* Chemosphere, 76, 952–958. doi: 10.1016/j.chemosphere.2009.04.026.

Keith, L.H., 2015. *The Source of U.S. EPA's Sixteen PAH Priority Pollutants.* Environmental Contamination and Toxicology, 35, 147–160. doi: 10.1080/10406638.2014.892886.

Kim, P.M., DeBoni, U. and Wells, P.G., 1997. *Peroxidase-Dependent Bioactivation and Oxidation of DNA and Protein in Benzo[a]Pyrene-Initiated Micronucleus Formation.* Free Radical Bio. Med., 23, 579–596.

Kole, P.J., Löhr, A.J., Van-Belleghem, F. and Ragas, A., 2017. *Wear and Tear of Tyres: A Stealthy Source of Microplastics in the Environment.* Environmental Resaerch and Public Health, 14, 1265. doi: 10.3390/ijerph14101265.

Lampi, M.A., Gurska, J., MCDonald, K.I.C., Xie, F., Huang, X., Dixon, D.G. and Greenberg, B.M., 2006. *PHOTOINDUCED TOXICITY OF POLYCYCLIC AROMATIC HYDROCARBONS TO DAPHNIA MAGNA: ULTRAVIOLET-MEDIATED EFFECTS AND THE TOXICITY OF POLYCYCLIC*

AROMATIC HYDROCARBON PHOTOPRODUCTS. Environmental Toxicology and Chemistry, 25, 1079–1087. doi: 10.1897/05-276r.1.

Lassen, C., Hansen, S.F., Magnusson, K., Norén, F., Hartmann, N.I.B., Jensen, P.R., Nielsen, T.G. and Brinch, A., 2015. *Microplastics - Occurrence, effects and sources of releases to the environment in Denmark*. The Danish Environmental Protection Agency.

Lin, J., Yan, D., Fu, J., Chen, Y. and Ou, H., 2020. *Ultraviolet-C and vacuum ultraviolet inducing surface degradation of microplastics*. Water Research, 186, 116360. doi: 10.1016/j.watres.2020.116360.

Lu, F., Su, Y., Ji, Y. and Ji, R., 2021. *Release of Zinc and Polycyclic Aromatic Hydrocarbons From Tire Crumb Rubber and Toxicity of Leachate to Daphnia magna: Effects of Tire Source and Photoaging*. Bulletin of Environmental Contamination and Toxicology, 107, 651–656. doi: 10.1007/s00128-021-03123-9.

Magnusson, K., 2014. *Mikroskräp i Avloppsvatten Från tre Norska Avloppsreningsverk*. IVL Svenska Miljöinstitutet: Stockholm, Sweden.

Magnusson, K. and Wahlberg, C., 2014. *Mikroskopiska Skräppartiklar i Vatten Från Avloppsreningsverk*. IVL Svenska Miljöinstitutet: Stockholm, Sweden.

Marsili, L., Coppola, D., Blanchi, N., Maltese, S., Bianchi, M. and Fossi, M.C., 2014. *Release of Polycyclic Aromatic Hydrocarbons and Heavy Metals from Rubber Crump in Synthetic Turf Fields: Preliminary Assessment for Athletes*. Environmental and Analytical Toxicology, 5, 952–958. doi: 10.4172/2161-0525.1000265.

Martinez, J.D., Puy, N., Murillo, R., Garcia, T., Navarro, V. and Mastral, A.M., 2013. *Waste Tyre pyrolosis - A review*. Renewable and Sustainable Energy Reviews, 23, 179–213. doi: 10.1016/j.rser.2013.02.038.

Miljøstyrelsen, 2016. *Zink (CAS nr. 7440-66-6). Fastsættelse af vandkvalitetskriterier*. `https://mst.dk/media/196589/zink-7440-66-6.pdf`. Downloaded: 05-05-2022.

Miljøstyrelsen, 2021. *BEK nr 2361 af 26/11/2021, Drikkevandsbekendtgørelsen*. `https://www.retsinformation.dk/eli/lta/2021/2361`. Downloaded: 05-05-2022.

Murphy, F., Ewins, C., Carbonnier, F. and Quinn, B., 2016. *Wastewater Treatment Works (WwTW) as a Source of Microplastics in the Aquatic Environment*. Environmental Science and Technology, 50, 5800–5808. doi: 10.1021/acs.est.5b05416.

Muyssen, B.T.A. and Janssen, C.R., 2001. *Zinc acclimation and its effect on the zinc tolerance of Raphidocelis subcapitata and Chlorella vulgaris in laboratory experiments*. Chemosphere, 45, 507–514. doi: 10.1016/s0045-6535(01)00047-9.

Naderi, K.V., Bustillo-Lecompte, C.F., Mehrvar, M. and Abdekhodaie, M.J., 2017. *Combined UV-C/H2O2-VUV processes for the treatment of an actual slaughterhouse wastewater*. Journal of Environmental Science and Health, 52, 314–325. doi: 10.1080/03601234.2017.1281650.

Nilsson, N.H., Feilberg, A. and Pommer, K., 2005. *Emissions and evaluation of health effects of PAH's and aromatic mines from tyres.* Danish Ministry of the Environment, Survey of Chemical Substances in Consumer Products, 54.

Patel, A.B., Shaikh, S., Jain, K.R., Desai, C. and Madamwar, D., 2020. *Polycyclic Aromatic Hydrocarbons: Sources, Toxicity and Remediation Approaches.* Frontiers in Microbiology, 11, 562813. doi: 10.3389/fmicb.2020.562813.

PlasticsEurope, cited October 2021. *Annual production of plastics worldwide from 1950 to 2020.*

Polyakova, O.V., Mazur, D.M., Artaev, V.B. and Lebedev, A.T., 2013. *Determination of Polycyclic Aromatic Hydrocarbons in Water by Gas Chromatography/Mass Spectrometry with Accelerated Sample Preparation.* Journal of Analytical Chemistry, 68, 1099–1103. doi: 10.1134/S106193481313008X.

REACH, 2009. *COMMISSION REGULATION (EC) No 552/2009 of 22 June 2009 amending Regulation (EC) No 1907/2006 of the European Parliament and of the Council on the Registration, Evaluation, Authorisation and Restriction of Chemicals (REACH) as regards Annex XVII.* Official Journal of the European Union.

Rhodes, E., Ren, Z. and Mays, D., 2012. *Zinc Leaching from Tire Crumb Rubber.* Environmental Science and Technology, 46, 12856–12863. doi: 10.1021/es3024379.

Rosinska, A., 2021. *The influence of UV irradiation on PAHs in wastewater.* Journal of Environmental Management, 293, 112760. doi: 10.1016/j.jenvman.2021.112760.

Schmidt, R., Griesbaum, K., Behr, A., Biedenkapp, D., Voegs, H.W., Garbe, D., Paetz, C., Collin, G., Mayer, D. and Höke, H. Hydrocarbons. In *Ullmans Encyclopedia of Industrial Chemistry.* Wiley, 2015. doi: 10.1002/14356007.a13_227.pub3.

Simon, M., Hartmann, N.B. and Vollertsen, J., 2021. *AcceleratedWeathering Increases the Release of Toxic Leachates from Microplastic Particles as Demonstrated through Altered Toxicity to the Green Algae Raphidocelis subcapitata.* Toxics, 9, 185. doi: 10.3390/toxics9080185.

Song, Y.K., Hong, S.H., Jang, M., Han, G.M., Jung, S.W. and Shim, W.J., 2017. *Combined Effects of UV Exposure Duration and Mechanical Abrasion on Microplastic Fragmentation by Polymer Type.* Environmental Science and Technology, 51, 4368–4376. doi: 10.1021/acs.est.6b06155.

Stevenson, K., Stallwood, B. and Hart, A.G., 2008. *Tire Rubber Recycling and Bioremediation: A Review.* Bioremediation Journal, 12, 1–11. doi: 10.1080/10889860701866263.

Supelco, 2021. *Programming Data for Spectroquant Test Kits Calibration Information: wavelength, slope and blank value.* Merck, `www.sigmaaldrich.com/photometry`.

Sørensen, L., Groven, A.S., Hovsbakken, I.A., Puerto, O.D., Krause, D.F., Sarno, A. and Booth, A.M., 2021. *UV degradation of natural and synthetic microfibers causes fragmentation of polymer degradation products and chemical additives.* Science of the Total Environment, 755, 1–9. doi: 10.1016/j.scitotenv.2020.143170.

Tang, Y., Sun, S., Zhang, L., Du, Z., Zhuang, J. and Pan, J., 2018. *Determination of 16 polycyclic aromatic hydrocarbons in tire rubber by ultra-highperformance supercritical fluid chromatography combined with atmospheric pressure photoionization-tandem mass spectrometry.* Analytical Methods, 10, 4902–4908. doi: 10.1039/c8ay01580e.

Unice, K.M., Kreider, M.L. and Panko, J.M., 2013. *Comparison of Tire and Road Wear Particle Concentrations in Sediment for Watersheds in France, Japan, and the United States by Quantitative Pyrolysis GC/MS Analysis.* Environmental Science and Technology, 47, 8138–8147. doi: 10.1021/es400871j.

Unice, K.M., Weber, M.P., Abramson, M.M., Reed, R.C.D, van Gils, J.A.G. and Markus, A.A., 2019. *Characterizing export of land-based microplastics to the estuary - part I: application of integrated geospatial microplastic transport models to assess tire and road wear particles in the Seine watershed.* Science of the Total Environment, 646, 1639–1649. doi: 10.1016/j.scitotenv.2018.07.368.

Verschoor, A.J., 2015. *Towards a definition of microplastics Considerations for the specification of physico-chemical properties.* RIVM letter report, 0116, 1–38.

Wernersson, A.S. and Dave, G., 1997. *Phototoxicity Identification by Solid Phase Extraction and Photoinduced Toxicity to Daphnia magna.* Environmental Contamination and Toxicology, 32, 268–273. doi: 10.1007/s002449900184.

WHO, 2016. *Radiation: Ultraviolet (UV) radiation.* World Health Organization, `https://www.who.int/news-room/questions-and-answers/item/radiation-ultraviolet-(uv)`.

Wik, A., 2007. *Toxic Components Leaching from Tire Rubber.* Bull Environ Contam Toxicol, 79, 114–119. doi: 10.1007/s00128-007-9145-3.

Wik, A. and Dave, G., 2006. *Acute toxicity of leachates of tire wear material to Daphnia magna—Variability and toxic components.* Chemosphere, 64, 1777–1784. doi: 10.1016/j.chemosphere.2005.12.045.

Wik, A., Nilsson, E., Kallqvist, T., Tobiesen, A. and Dave, G., 2009. *Toxicity assessment of sequential leachates of tire powder using a battery of toxicity tests and toxicity identification evaluations.* Chemosphere, 77, 922–927. doi: 10.1016/j.chemosphere.2009.08.034.

Yang, L., Li, M., Li, W., Jiang, Y. and Qiang, Z., 2018. *Bench- and pilot-scale studies on the removal of pesticides from water by VUV/UV process.* Chemical Engineering Journal, 342, 155–162. doi: 10.1016/j.cej.2018.02.075.

Zewde, A.A., Li, Z., Zhang, L., Odey, E.A. and Xiaoqin, Z., 2020. *Utilisation of appropriately treated wastewater for some further beneficial purposes: a review of the disinfection method of treated wastewater using UV radiation technology.* Reviews on Environmental Health, 35, 139–146. doi: 10.1515/reveh-2019-0066.

Zhang, K., Hamidian, A.H., Tubic, A., Zhang, Y., Fang, J.K.H, Xu, C. and Lam, P.K.S., 2021. *Understanding plastic degradation and microplastic formation in the environment: A review.* Environmental Pollution, 274, 116554. doi: 10.1016/j.envpol.2021.116554.

Zoschke, K., Bornick, H. and Worch, E., 2014. *Vacuum-UV radiation at 185 nm in water treatment - A review.* Water Research, 52, 131–145. doi: 10.1016/j.watres.2013.12.034.

Heraeus

Strahler NIQ 40/18

Niederdruck VUV Strahler / Low pressure VUV lamp
Artikelnummer / part number: 45000024

Es wird ein Komma als Dezimalzeichen und ein Punkt als Tausender-Trennungszeichen verwendet. / The comma is used as decimal marker and the dot as thousands separator.

Elektrische Daten / electrical data:

▪ Lampenstrom / lamp current:	1,40 A
▪ Lampenspannung / lamp voltage:	32 V
▪ Lampenleistung / lamp input:	44 W
▪ Anschlussleistung / power input:	55 W
▪ Anschlussstrom / mains current:	0,38 A
▪ Anschlussspannung / mains voltage *:	230 V
▪ Vorschaltgeräte Typ / ballast type:	ZED 40-60W

*abhängig vom EVG Typ / depending on ECG type
Betrieb nur mit EVG / operation only with electronic ballast

Skizze nicht maßstabgerecht /drawing not to scale

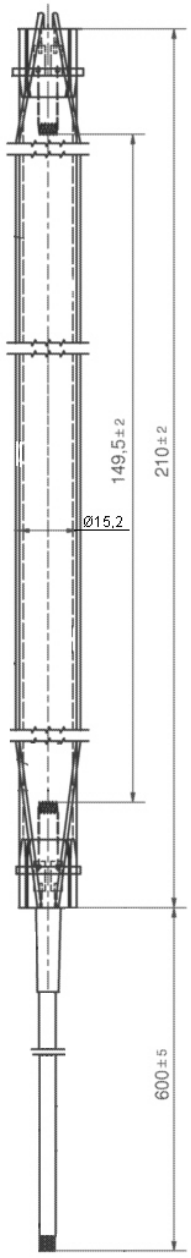

Betriebsweise / operating conditions:

▪ Kühlung / cooling *:	Konvektionskühlung
▪ Brennlage / operating position:	optional
▪ Leuchtrohrtemperatur / tube temperature:	<130℃
▪ Leuchtrohrdurchmesser / Outer diameter:	15,20 mm

Strahlungsphysikalische Daten / radiation data:

▪ Strahlungsfluss / radiation flux at 185 nm:	4 W

freibrennend bei / in air at temperature 40-80℃

Lebensdauer / lifetime:

Abhängig von der Betriebsweise / depending on operating conditions

- Erwartete Nutzlebensdauer / expected useful life time: 8.000 h
- Intensitätsrückgang: 50 % bei 185 nm nach 8.000 h – Bezug 100 h Wert. / Intensity decrease: 50 % at 185 nm after 8.000 h – based on 100 h value.

Diese Angaben sind typische Mittelwerte und unter Laborbedingungen ermittelt. / These data are typical mean values measured under laboratory conditions.

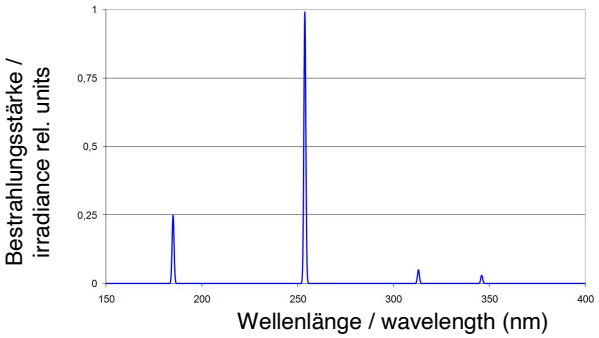

Stromlaufplan / circuit diagram

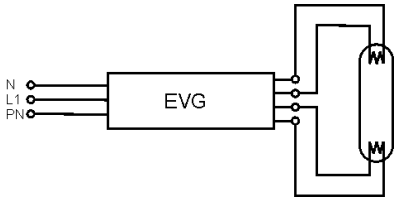

Heraeus Noblelight behält sich vor, Abbildungen und technische Daten in diesem technischen Datenblatt zu ändern. Es gilt die jeweils aktuelle Version des technischen Datenblattes. Es obliegt der Verantwortung des Kunden zu prüfen, ob ihm die aktuelle Version des Technischen Datenblattes vorliegt. / Heraeus Noblelight reserves the right to change drawings and technical data in this Technical Data Sheet. The latest updated version of the Technical Data Sheet is prevailing. It is within the responsibility of the customer to check whether the latest updated version of the Technical Data Sheet is available to him.

.

Germany
Heraeus Noblelight GmbH
Heraeusstraße 12-14
63450 Hanau, Germany
Phone +49(0)6181.35-9925
Fax +49(0)6181.35-9926
hng-disinfection@heraeus.com
www.heraeus-noblelight.com

Appendix 2: Modelled inhibition curves for UVC and VUV toxicity

UVC treatment of TRMP

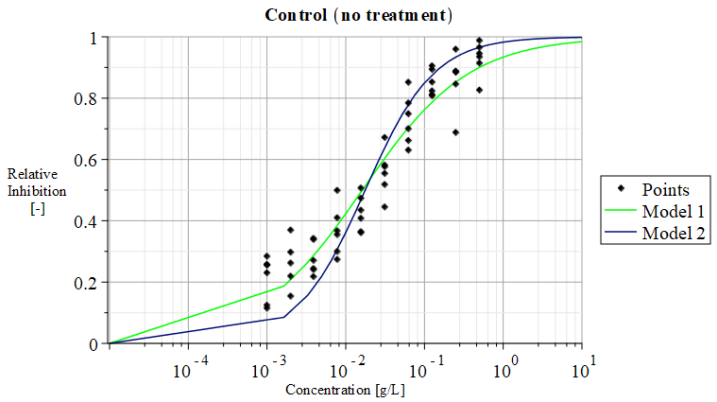

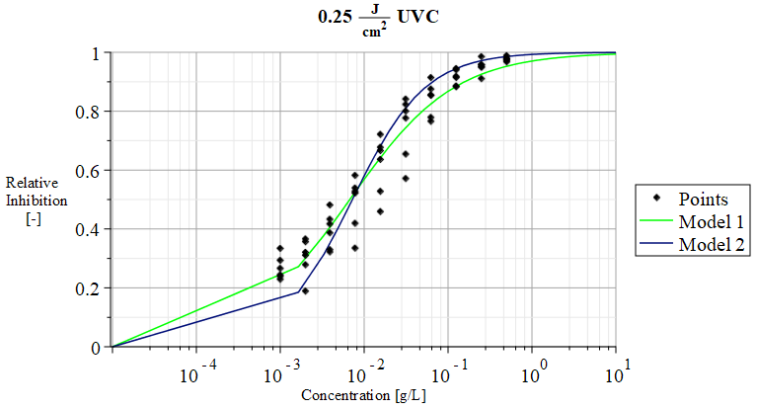

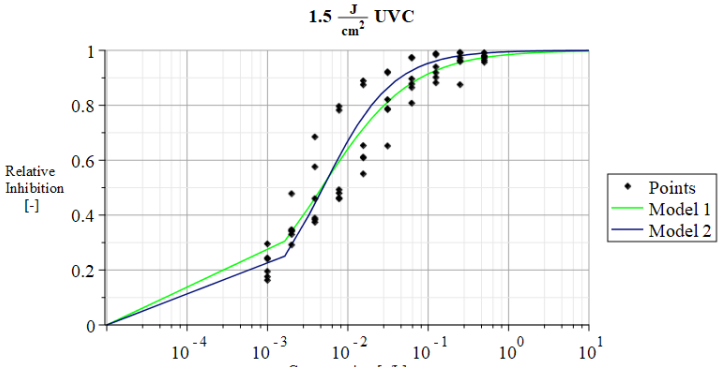

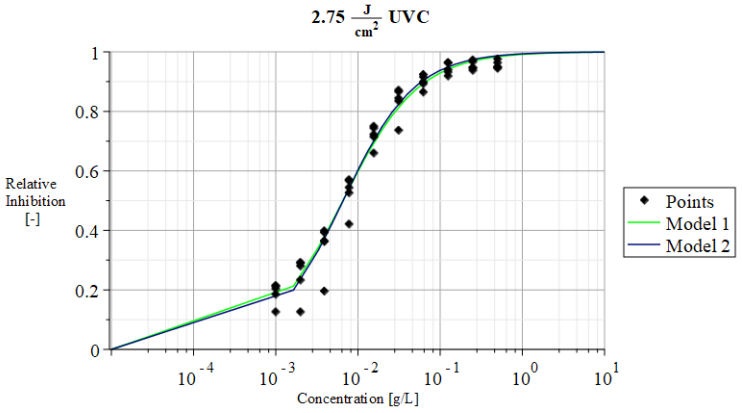

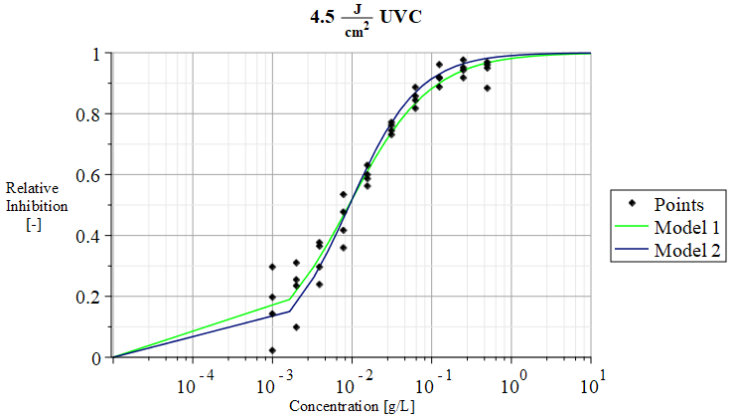

VUV+UVC treatment of TRMP

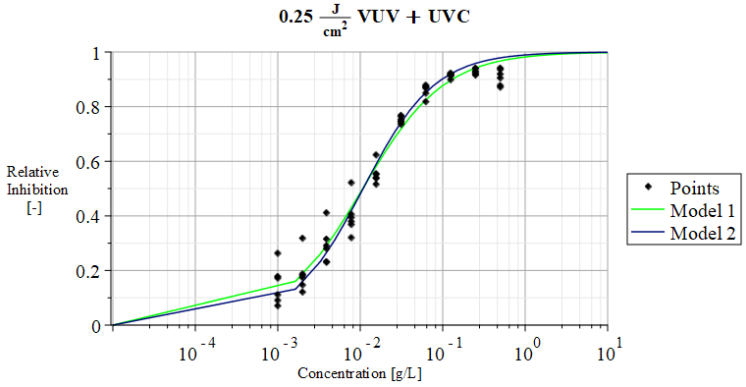

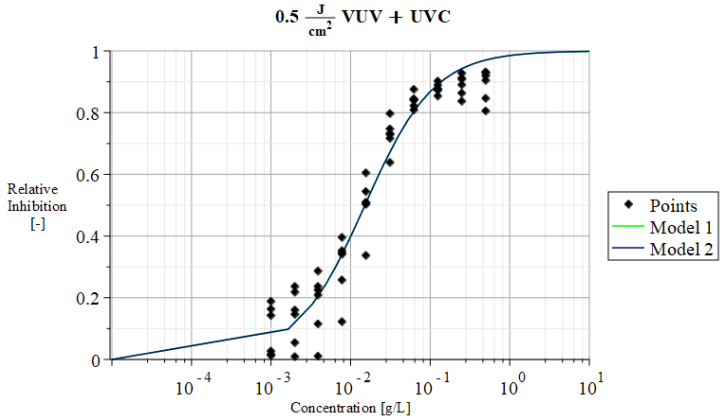

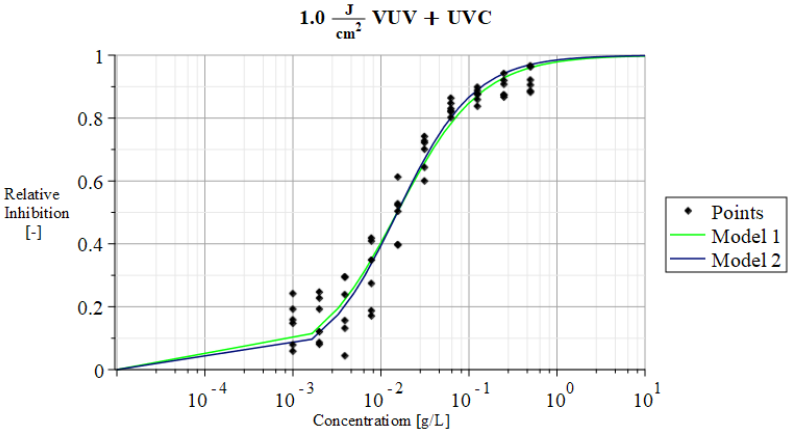

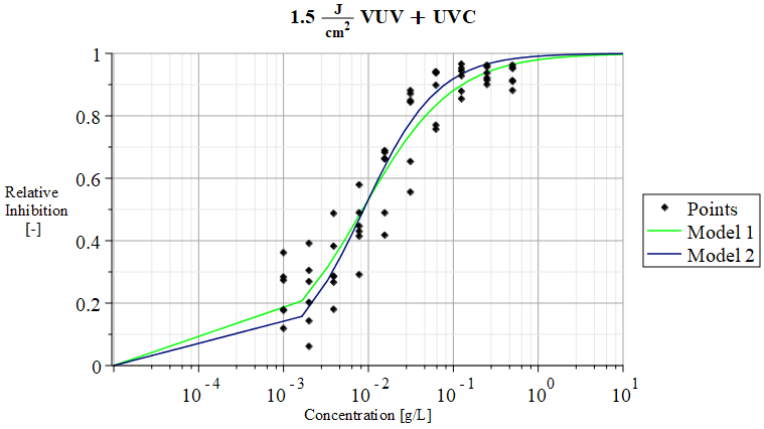

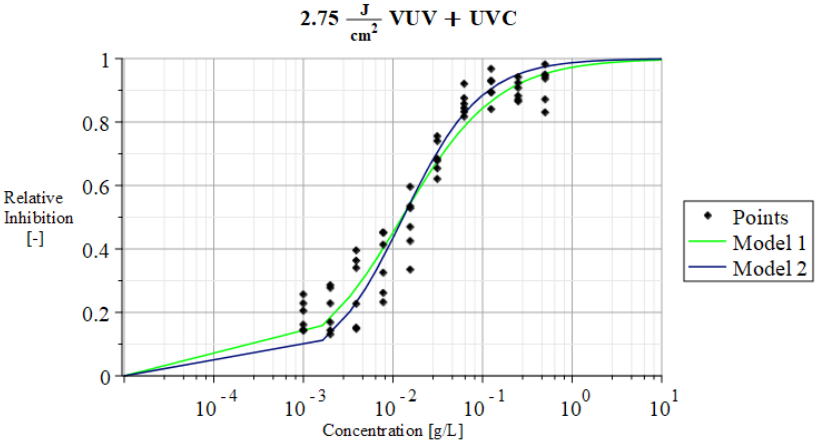

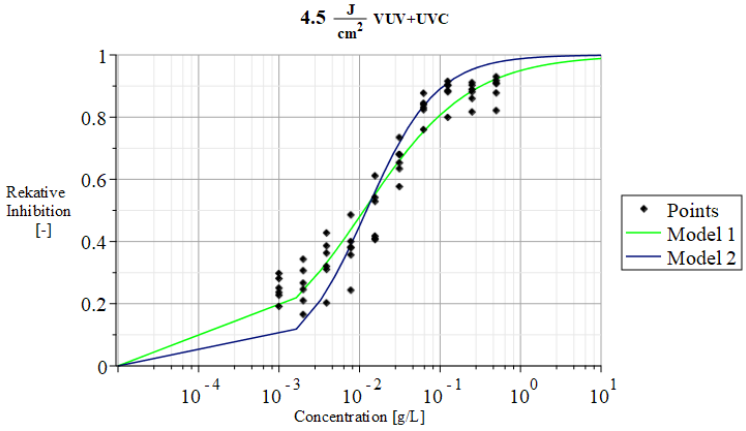

UVC treatment of supernatant

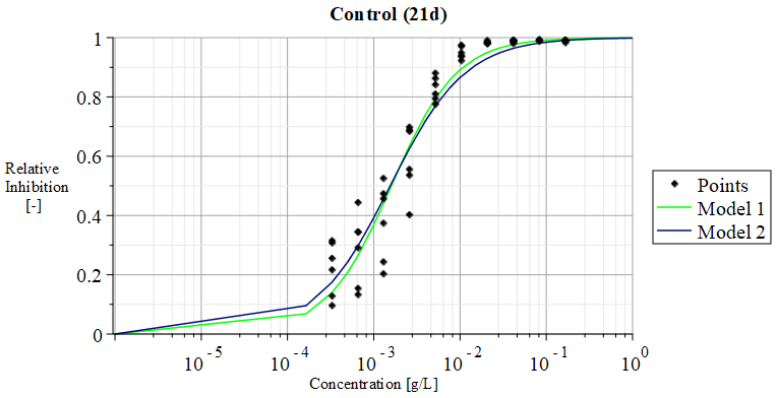

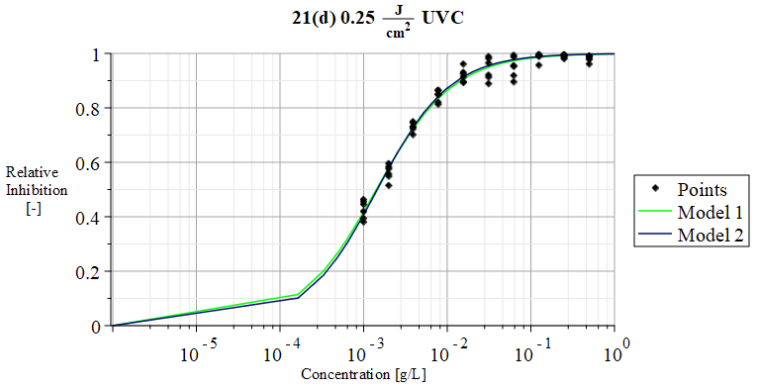

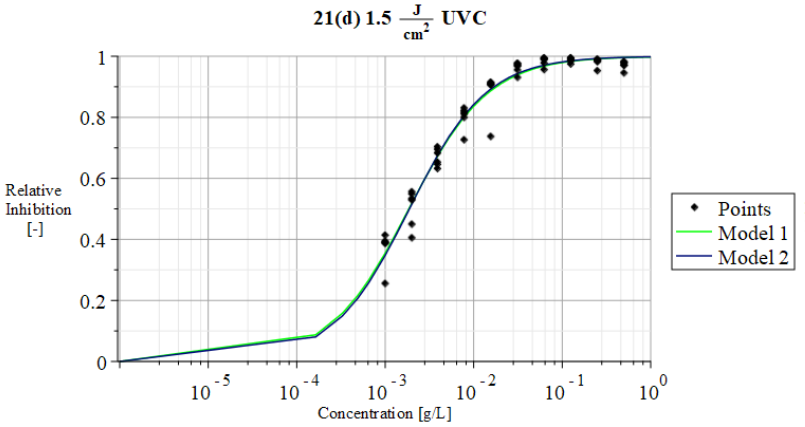

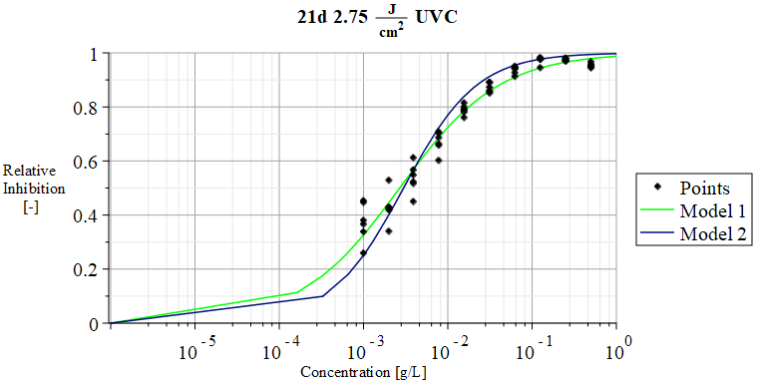

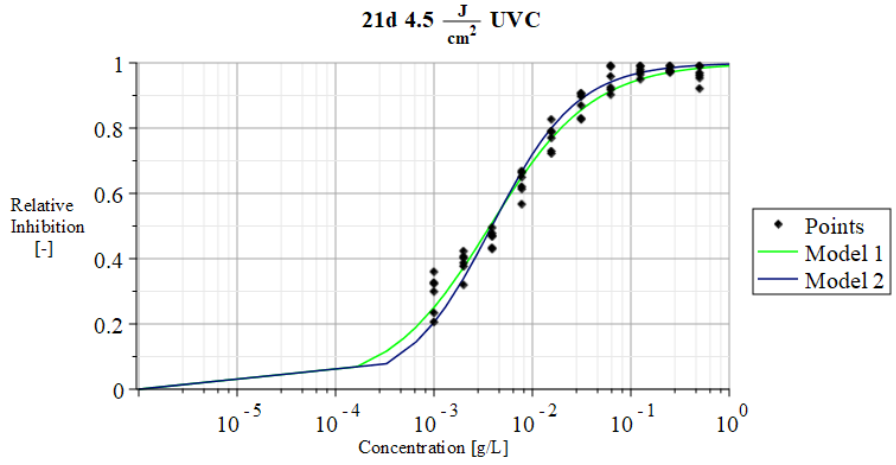

VUV+UVC treatment of supernatant